

UNIVERSITY OF NAPLES FEDERICO II

**DOCTORATE IN
MOLECULAR MEDICINE AND MEDICAL BIOTECHNOLOGY**

XXXIII CYCLE



Mariella Cuomo

**DNA methylation dynamics at genes specific level
during brain development and in schizophrenia**



Year 2021

UNIVERSITY OF NAPLES FEDERICO II

**DOCTORATE IN
MOLECULAR MEDICINE AND MEDICAL BIOTECHNOLOGY**

XXXIII CYCLE



**DNA methylation dynamics at genes specific level
during brain development and in schizophrenia**

Tutor
Prof. Lorenzo Chiariotti

Candidate
Mariella Cuomo

Year 2021

Index

Abbreviations.....	5
Abstract.....	6
1 - Background	8
1.1 Epigenetic mechanisms	8
1.2 DNA methylation dynamics	12
1.3 Cell to Cell heterogeneity and the epialleles analysis	14
1.4 DNA methylation in brain development and in neuropsychiatric disorders	16
1.5 The role of D-amino acids in brain development and in schizophrenia..	20
1.6 DNA methylation at genes encoding enzymes involved in D-amino acids metabolism.	22
2 - Aim of thesis	23
3 – Materials and methods	25
3.1 Collection of mouse brain tissue	25
3.2 Isolation of neurons, astrocytes, and enriched microglia/ oligodendrocyte/endothelial cells	25
3.3 Human Tissue Samples Collection.....	27
3.4 DNA and RNA extraction protocols	27
3.5 cDNA and Real Time experiments.	27
3.6 Bisulfite and oxidative bisulfite treatment	28
3.7 Amplicon Library preparation	29
3.8 Sequence handling and bioinformatics analyses	31
3.9 Statistical analyses.....	33
4 – Results	34
4.1 The different applied methods to study DNA methylation	34
4.2 Epigenetic landscape of genes involved D-Ser and D-Asp metabolism during brain development in mice	37
4.2.1 D-Asp and D-Ser levels in hippocampus, cortex and cerebellum of mice during development	37
4.2.2 DAO and DDO gene structures in mice	39
4.2.3 DNA methylation and mRNA expression levels at DAO promoter in Hippocampus, Cerebellum and Cortex during brain development	41

4.2.4 Analysis of 5-mCpG and 5-hmCpG dynamics at DAO promoter region	44
4.2.5 DNA methylation dynamics in cerebellar astrocytes and neurons during the P1-P15 temporal window	46
4.2.6 DNA methylation and mRNA expression of the DDO gene in different brain areas at different developmental stages	48
4.3 DNA methylation and mRNA expression scenario of DAO and DDO genes in post-mortem tissues from patients with schizophrenia	50
4.3.1 DAO and DDO gene structures in human	51
4.3.2 Analysis of DNA methylation and mRNA expression at DAO gene promoter in non-psychiatric subjects and patients with schizophrenia.	52
4.3.3 DDO promoter methylation and mRNA expression in non-psychiatric subjects and patients with schizophrenia.	54
4.4 Epiallele distribution analysis and epiallele classes analysis at DAO and DDO promoters in mice during brain development and in patients with schizophrenia	56
4.4.1 Epiallele distribution analysis in different brain areas during brain development.....	56
4.4.2 Spatio-temporal distribution of epialleles at DDO gene during mouse brain development	59
4.4.3 Single molecules DAO methylation analyses in non-psychiatric subjects and patients with schizophrenia.....	61
4.4.4 Single molecules DDO methylation analyses in non-psychiatric subjects and patients with schizophrenia.....	63
5 – Discussion.....	65
6 – Conclusions	68
Acknowledgements.....	70
References	71
List of Publications.....	87

Abbreviations

DAO:	D-Aminoacid oxidase
DDO:	D-Aspartate oxidase
CpG:	Cytosine-phosphate-Guanine
ncRNA:	Noncoding RNA
siRNA:	Small interfering RNA
piRNA:	Piwi-interacting RNA
DNA:	Deoxyribonucleic Acid
DNMT:	DNA methyl transferase
TET:	Ten Eleven Translocation
RNA:	Ribonucleic Acid
PCR:	Polymerase Chain Reaction
NGS:	Next generation sequencing
Ct:	Threshold cycle
HIPP:	Hippocampus
CX:	Cortex
DLPFC:	Dorsolateral Prefrontal Cortex
CB:	Cerebellum
HDAC:	Histone Deacetylase
HAT:	Histone Acetyltransferase
KMT:	Histone Methyltransferase
SET:	Su(var)3-9, Enhancer-of-zeste and Trithorax
SAM:	S-Adenosyl Methionine
MecP2:	Methyl-CpG binding Protein 2
MBD1:	Methyl-CpG-Binding Domain protein 1
PGC:	Primordial Germ Cells
mCpG:	methyl-Cytosine-phosphate-Guanine
hmCpG:	hydroxymethyl-Cytosine-phosphate-Guanine
PRDM1:	PR/SET Domain 1
PRDM14:	PR/SET Domain 14
UHRF1:	Ubiquitin Like with PHD And Ring Finger Domains 1
CpH:	Cytosine-phosphate-other nucleotides
NMDA:	N-methyl-D-aspartate
NMDAr:	N-methyl-D-aspartate receptor
D-Ser:	D-Serine
D-Asp:	D-Aspartate

Abstract

Defined epigenetic modifications occurring during brain development may play a fundamental role on brain function. An alteration in the establishment of correct DNA methylation at specific genes has been associated with neuropsychiatric disorders. In this regard, during perinatal period DNA methylation may finely control genes regulating brain levels of critical neuromodulators such as D-Serine and D-Aspartate. Since levels of these D-amino acids have been found altered in some mental disorders such as schizophrenia, the lack of an epigenetic control may contribute to the genesis and/or progression of these diseases. Thus, during my PhD, I performed a comprehensive DNA methylation analysis along with mRNA expression at DAO and DDO genes, involved in the degradation of D-Serine and D-Aspartate, respectively. I performed the analyses in mice during development and in post-mortem tissues of patients with schizophrenia. I evaluated DNA methylation using amplicon bisulfite sequencing on Illumina MiSeq platform and I also performed an in-depth single molecule methylation approach in order to assess the cell to cell methylation heterogeneity. I found strong spatiotemporal changes in DNA methylation at the DAO gene during development, especially in cerebellar astrocytes and particularly at two specific CpG sites. These CpGs at DAO gene promoter showed high degree of hydroxymethylation at post-natal day 1 and at, post-natal day 15 the global levels of DNA methylation AND hydroxymethylation dramatically decreased. This demethylation strongly activated DAO gene expression, indirectly promoting the physiological degradation of cerebellar D-serine. The same mechanisms emerged at DDO promoter in cerebellum, where two CpG sites were demethylated during development activating the expression of the gene. Furthermore, both in mouse brain during development and in post-mortem brain tissues, the applied single-molecule methylation approach demonstrated that epiallele distribution was able to detect differences in DNA methylation representing area-specific methylation

signatures, which are likely not detectable with targeted or genome-wide methylation analyses. The present study demonstrates that D-Serine and D-Aspartate levels during brain development are indirectly regulated by DNA methylation that govern the expression of DAO and DDO genes. Furthermore, single-molecule methylation approach promises to identify different cell-type composition and function in different brain areas and developmental stages. Overall, these analyses demonstrate that at selected genes, epiallele-based analyses may be very informative and can be successfully utilized in a broad range of applications, including in depth determination of epigenetic origin of brain diseases.

1. Background

1.1 Epigenetic mechanisms

The term “epigenetics” was coined for the first time by Waddington in 1942. He defined the epigenetics as a branch of biology studying the changes in phenotype without altering the genotype. He used the expression "epigenetic landscape" as a metaphor for biological development. In fact, Waddington postulated that cell fate is established during development and cells are like marbles that reach their lowest point by randomly rolling in the valleys separated by the crests (Goldberg AD et al., 2007; Jaenisch R et al., 2003; Holliday et al., 2006). Indeed, most cell differentiation processes are based on epigenetic phenomena (Henikoff S et al., 1997; Gökbuget D et al., 2019; Boland MJ et al., 2014). The cells of a multicellular organism derive from a single cell and so they have the same genetic heritage. However, they develop differently generating more than 100 different cell types. During morphogenesis, pluripotent stem cells become highly differentiated cells, thanks to the activation or repression of specific sets of genes (Theunissen TW et al., 2017). Thereafter, epigenetics was used to explain the complexity of multicellular organisms in term of transcriptional heterogeneity. Indeed, cells in different tissues can achieve different function by maintaining distinct gene expression profiles. This cellular heterogeneity is ensured by three main epigenetic mechanisms: DNA methylation (Deaton AM et al., 2011), chromatin modification (Quina AS et al., 2006; Strahl BD et al., 2000) and non-coding RNA (Mohammad F et al., 2012; Kaikkonen MU et al., 2011) (Figure 1). Chromatin is the combination between DNA and histone proteins. Depending on the structure of DNA-histone complex, gene expression can be regulated modulating access to transcription factors and transcriptional machinery. The core of the chromatin is the nucleosome, an octamer composed by two heterodimers H2A and H2B and an H3-H4 tetramer around which DNA wraps. From the nucleosome, histones

expose tails that, especially those of H3 and H4, are susceptible to numerous post-translational modifications, such as methylation, acetylation, phosphorylation, ubiquitination, biotinylation, sumoylation. All these modifications ensure chromatin variability (Jenuwein T et al., 2001). The most common and known histone modifications are acetylation and methylation. In general, acetylation of histones consists in the transfer of an acetyl group onto a lysine residue. This modification is achieved by histone acetyltransferase (HAT) and can be reversed by histone deacetylases (HDAC) (Yang XJ et al., 2007; Kouzarides T, 2007). Histone acetylation neutralizes the positive charges of lysine residues and reduces the binding strength between histones and DNA, causing changes in the structural organization of chromatin (Allfrey V et al., 2007). Therefore, acetylation opens the chromatin structure by promoting the binding of the factors necessary for gene transcription: hyperacetylation is associated with an active transcription state, hypoacetylation is related to transcriptional repression (Becker PB, 1994). Histone methylation can generally occur at lysine and arginine residues. Lysine methylation is catalyzed by lysine methyltransferase (KMT) and lysines can be mono-, di- and trimethylated. All KMTs have a SET domain, containing the catalytic site, and the site for the binding of the cofactor S-adenosylmethionine (SAM), donor of the methyl group. According to the number of methyl-group and the position of the lysine, histone methylation may have a different and opposite role in the regulation of transcription (Hyun K, 2017). Given the wide complexity in the histone modifications establishment, it is not possible to identify a precise histone code associated to gene activation or repression. Another class of epigenetics regulators are the non-coding RNA (ncRNA) (Derrien et al., 2012; Mattick JS et al., 2006). Several recent studies have shown that ncRNAs are involved in the regulation of a wide range of biological processes, such as cell cycle regulation (Mens MMJ et al., 2018), pluripotency (Yan P et al., 2017), differentiation (Fatica A et al., 2014) and cell death (Feng Q et al., 2019). They are functional RNA molecules that are transcribed from DNA but not translated into proteins.

They include siRNA, piRNA, miRNA, and lncRNA. It has also been demonstrated that the short and long non-coding RNA are implicated in several epigenetic processes, such as heterochromatin formation, DNA methylation targeting, gene silencing and histone modification (Wang KC et al., 2011). The ncRNAs can regulate chromatin states by recruiting chromatin remodeling complexes either in genomic loci that are close to their transcription site (cis regulation) or at distant genomic loci (trans regulation). At the transcriptional level, ncRNAs may bind the promoter of specific genes and prevent access to transcription factors by inhibiting the transcription. DNA methylation is the most studied epigenetic mechanism generally associated to gene silencing and heterochromatin formation (Jones PA, 2012; Breiling A et al., 2015; Raiber EA et al., 2017; Razin A et al., 1980). It consists in the covalent addition of a methyl group on the 5' of cytosine residues with the formation of 5-methylcytosines (Adams RLP, 1990). DNA methylation generally occurs at CpG dinucleotide, even though recent evidences have shown the existence of non-CpG methylation, especially in brain tissue and in stem cells (Patil V et al., 2014; Guo W et al., 2016). The reaction is catalyzed by a class of enzymes defined DNA methyltransferases (DNMTs) that use the cofactor SAM as a donor of the methyl group (Okano M et al., 1998; Yen RW et al., 1992). There are two classes of DNMT in mammals: DNMT1, also defined the "*maintenance*" methyltransferase, that is involved in the methylation of hemi-methylated nascent DNA (Leonhardt et al., 1992; Liu et al., 1998), and DNMT3, consisting in three members DNMT3a, DNMT3b and DNMT3L, that instead establish "*de-novo*" methylation patterns in the early stages of embryonic development and in germ cells (Okano et al., 1999). DNMT3 enzymes also play a role in maintaining DNA methylation in heterochromatic regions. DNMT3a and DNMT3b are expressed in embryonic tissues and undifferentiated embryonic stem cells, while their expression is down regulated in differentiated cells (Uysal F et al, 2017). The third member of the family is DNMT3L, which does not possess the catalytic domain, but seems to be a key regulatory factor during gametogenesis

and embryogenesis (Veland N et al., 2019). Mutations in DNMT1 or DNMT3a/3b genes in mouse germlines block development and cause lethality of the embryos, suggesting that DNMTs play crucial roles in embryogenesis (Chen T et al., 2003; Liao J et al., 2015)

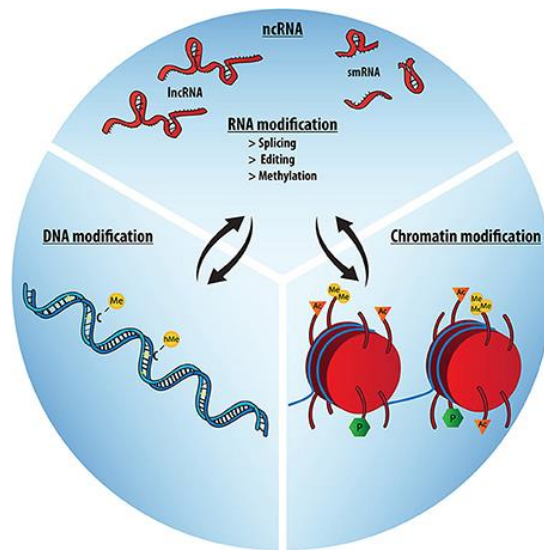


Figure 1. Epigenetic mechanism. Schematic representation of epigenetic modifications explained in the text.

1.2 DNA methylation dynamics

Despite some tissue-specific differences, mammalian genomes present a high degree of DNA methylation and the 70–80% of CpG dinucleotides are methylated (Xin Y et al., 2011). DNA methylation is, in fact, involved in several biological processes, such as genomic imprinting (Weaver JR et al., 2009), X chromosome inactivation (Cotton AM et al., 2011) and has a key role in development (Zeng Y et al., 2019; Smith ZD et al., 2013; Bird A, 2002).

The effect of DNA methylation on development is explicated through its regulatory role in gene expression. Methylation-mediated gene regulation may occur through two mechanisms: (i) CpG methylation directly interfere with the binding of certain transcription activators within the transcription factor binding domain (Zhu H et al., 2016; Jin J et al., 2016); (ii) specific methyl-CpG binding proteins such as MeCP2 and MBD1 may act as transcriptional repressors themselves binding the methylated DNA and silencing the genes (Fan G et al., 2005; Kribelbauer JF et al., 2019). The methyl-CpG binding proteins are also able to recruit several other complexes, such as histone deacetylase, histone methylase and chromatin remodeling complexes, resulting in transcriptional repression and heterochromatin formation (Clouaire T et al., 2008). However, DNA methylation is not a stable and fixed modification. Recently, another family of proteins have raised increasing interest, the Ten Eleven Translocation (TET) proteins (Wu X et al., 2017; Williams K et al., 2011;). TET enzymes act by catalyzing the oxidation of a residue of 5-methylcytosine (5-mC) to 5-hydroxymethylcytosine (5-hmC). The 5-hmC is the first step for the active DNA demethylation process. The discovery of this cytosine modification suggested that DNA methylation is a very dynamic process and the demethylation machinery is as important as the one that establish the 5-mC. In fact, in brain, 5-hmC seems to be very abundant, especially in neurons, and it was shown to be essential for the correct brain development (Rasmussen KD et al., 2016; Pfeifer GP et al., 2013). It has been widely demonstrated that the loss of TET enzymes

compromise proper differentiation of embryonic stem cells (Dawlaty MM et al., 2014; Reimer M Jr et al., 2019; Santiago M et al., 2014). All the mechanisms described above indicate that the continuous dynamic oscillation of methylation and demethylation events is likely essential for the correct development of mammals and only at the end of this modelling process, each type of cells will acquire a cell type-specific methylation profile becoming able to regulate the exact gene expression program. The dynamics of methylation is schematized in Figure 2.

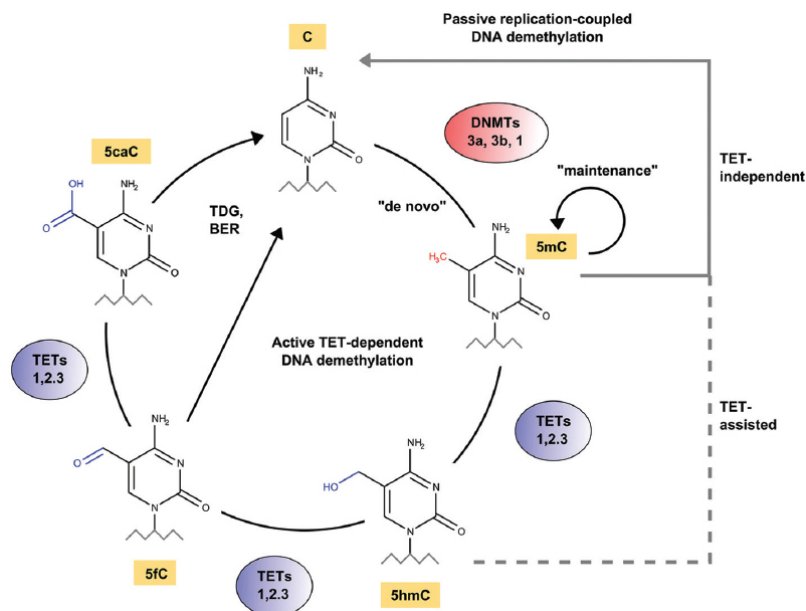


Figure 2. DNA methylation and demethylation process. Cytosine (indicated with C in the figure) can be modified in 5' position by DNMTs protein to become 5'-methylcytosine (5mC). The methyl group can be removed by two different mechanisms: a passive demethylation process, independent by TET enzymes and due to the replication of the cells, or by an active process, mediated by TETs through the conversion of 5-mC in 5-hydroxymethylcytosine (5hmC), 5-formylcytosine (5fC) and 5-carboxycytosine (5caC). The final removal of carboxyl group is committed to TDG or BER enzymes. (From Meier K and Recillas-Targa F, *New insights on the role of DNA methylation from a global view*, 2017)

1.3 Cell to Cell heterogeneity and the epialleles analysis

The vast majority of studies addressing a role to DNA methylation in regulating gene expression, regardless of the employed techniques, took into consideration the average amount of CpGs methylation in specific genomic regions or their genome-wide distribution with only relatively high resolution. However, mammalian genome contains about 29 millions of CpG sites (Fouse SD et al., 2010) which are non-randomly distributed along the genome and the methylation status of each of these CpG sites may be influenced by the methylation of the neighbor CpGs (Affinito et al., 2016). Thus, the epigenetic information retained by the DNA methylation at a gene promoter should be considered as the combination of methylated and unmethylated status of each CpG site constituting the analyzed region. Expanding this concept to the genome, the number of possible combinations is too huge (108,700,000) and may be a very hard task, even if the analysis could enormously increase the potential information content of genomic DNA. However, all the possible methyl-CpG combinations may be verify more easily at a single gene locus. In principle, each cell may bear a specific combination of methylated CpG at specific loci that may reflect the origin of the cell and/or the functional state of a given gene (allele) in that cell. This introduce the concept of “epipolymorphism” which goes far beyond the identification of differentially methylated regions. In fact, cells may be considered an epigenetically heterogeneous population in which each combination of mCpG at a given locus represents a specific "epiallele". Such information is lost when the average methylation, even at single CpG sites, is evaluated. Some previous studies based on bisulfite sequencing revealed that different combinations of mCpG are present at given loci and are usually interpreted as the effect of stochastic methylation and demethylation events resulting in an average methylation degree which is then associated to gene activity. However, it should be taken into consideration that each of the detected methylation profile corresponds to

the configuration of a single allele in a single cell belonging to tissue cell mixture and accounting for cell to cell methylation variability. By genome-wide approaches, some works evaluated the methylation of few adjacent CpGs and have identified the cell to cell methylation variability in liver (Qu W et al., 2016), in leukemias (Li S et al., 2014) and in immortalized fibroblasts (Landan G et al., 2012) nicely describing the stochastic and clonal evolution of epialleles during carcinogenesis.

1.4 DNA methylation in brain development and in neuropsychiatric disorders

In mammals, a global genetic reprogramming takes place during embryonic development. During the temporal window from primordial germ cells (PGCs) to somatic cells, the epigenome of the zygote is reorganized in order to erase the parental epigenetics memory and facilitate the gametogenesis process (Borgel J et al., 2010; Popp C et al., 2010). PGCs originate from a hypermethylated epiblast and undergo extensive DNA demethylation process with a reduction of global methylation levels from 70% to about 4% (Guibert S et al., 2014). Global DNA demethylation in the germline is thought to occur as a result of a passive mechanism: after the specification of PGCs, two factors, PRDM1 and PRDM14 repress the expression of DNA methyltransferase 3A, 3B and E3 ubiquitin protein ligase UHRF1, so that both the maintenance of methylation levels and the new wave of methylation are apparently repressed during the proliferation of PGCs (Guibert S et al., 2014). During gametogenesis, DNA methylation is re-established through de novo methylation events that allow the proper formation of the fertilized oocyte. Then, another demethylation event occurs until the blastocyst formation, with the exception of the imprinted regions. At this time point, the blastocyst starts to differentiate and contextually, a de novo methylation is established at specific genes defining the somatic cell lineages (Hajkova P et al., 2002). The methylation events that establish during this time window are thought to be maintained throughout the life and an alteration in this mechanism has been associated with numerous neuropsychiatric diseases, such as schizophrenia and bipolar disorder. In fact, mice with a postnatal deletion of DNMT1 and DNMT3a or with a global deletion of methyl-CpG-binding protein 2 (MeCP2) show abnormal neural plasticity and cognitive deficits (Feng J et al., 2010; Moretti P et al., 2006). This suggests that DNA methylation is essential for correct brain development and function (Figure 3).

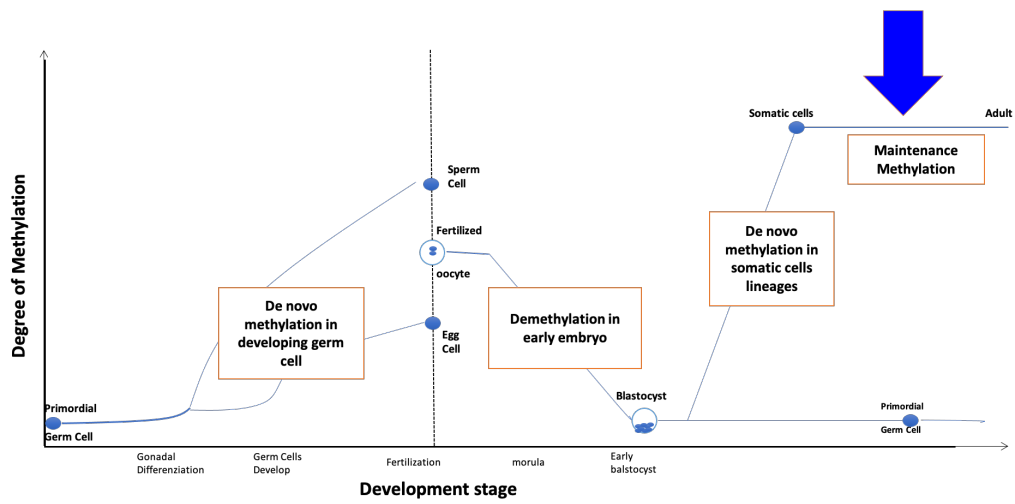


Figure 3. DNA methylation during development. Schematic representation of DNA methylation and demethylation events during development. On x-axis different developmental stages are reported while degree of methylation is indicated on y-axis.

During early neuronal differentiation, promoters of pluripotency-associated genes are silenced by de novo DNA methylation while genes related to neuronal pathways lose DNA methylation and start to be expressed (Mohn F et al., 2008). After birth, neuronal methylation profiles continue to evolve in parallel with developmental plastic changes (Lister R et al., 2013). One of the first works that reveal the key role of DNA methylation in brain development has been by Lister et al. They discovered that DNA methylation is able to distinguish two broad classes of cortical cells, neurons and astrocytes, since these cells show a distinct DNA methylation profile at specific gene sets. The progressive and well-orchestrated shaping of DNA methylation patterns in brain occur both at CpG and at non-CpG (CpH) sites. As a result, at genomic level each type of brain cells, despite sharing similar global mCpG content, acquire a cell-type specific DNA methylation landscape that gives an identity card for different brain cells and govern and stabilize an elected gene expression program (Florio et al., 2017). As said above, appropriate patterns of DNA methylation in the brain play an important role in mental health. Several pivotal gene-specific or genome-wide studies addressed a role to DNA methylation changes in animal models of neuropsychiatric disease or post-mortem brain of psychiatric subjects (Tsankova N et al., 2007; Keller S et al., 2010; Miller G, 2010; Perroud N et al., 2013; Nestler EJ et al., 2015; Labonté B et al., 2012). These studies revealed an alteration in average CpG methylation at certain important genes including several involved in glutamatergic and GABAergic neurotransmission, brain development, and other processes functionally linked to disease etiology (Mill et al., 2008). While the role of DNA methylation in neurodegenerative disorders such as Parkinson disease and Alzheimer disease has been broadly investigated (Wei X et al., 2020; Stoccoro A et al., 2018; Konki M et al., 2018) very few studies addressed an alteration in DNA methylation at selected genes in patients with schizophrenia (Jaffe AE et al., 2016; Li S et al., 2019; Hu TM et al., 2017). One of the most studied candidate genes displaying differential methylation in schizophrenia is reelin (RELN). Reelin has a crucial role in the extension of

axons and dendrites (Nabil Fikri RM et al., 2016) and it has been shown to participate in neuronal migration during early postnatal development (Hirota Y et al., 2017). Genetic studies have also suggested an association between RELN variants and schizophrenia (Marzan S et al., 2021; Costa E et al., 2020; Sozuguzel MD et al., 2019). RELN expression has been observed to be reduced between 30–50% in different brain areas in patients with schizophrenia (Beasley CL et al., 2020; Habl G et al., 2012). This reduction has been attributed to the hypermethylation of RELN promoter in post-mortem brain from patients with schizophrenia (Nabil Fikri RM et al., 2017).

1.5 The role of D-amino acids in brain development and in schizophrenia

In the central nervous system (CNS), two D-amino acids, D-serine and D-aspartate, occur in considerable concentrations, especially in specific stages of development (Kiriya Y et al., 2016; Hashimoto A et al., 1995). Both D-amino acids play important roles in development and functioning of mammalian brain and are produced and processed endogenously (Hashimoto A et al., 1997; Errico F et al., 2020; Errico F et al., 2012). D-Serine is a co-agonist of the N-methyl D-aspartate (NMDA) receptor and is relevant for its physiological activation (Schell MJ et al., 1995). Also D-Aspartate, an agonist of NMDAR, play a role in development and brain function (Katane M et al., 2012). As D-amino acids play biological roles, alterations in the concentrations of D-amino acids might occur in some neuropsychiatric disorders and relate to their pathogenesis. Dysregulation of D-aminoacids system has been suggested as a contributor in the genesis and progression of schizophrenia and other neuropsychiatric and neurodegenerative conditions (Verrall L et al., 2012; Coyle JT et al., 2012; Balu DT et al., 2015; Errico F et al., 2015; Hashimoto K et al., 2003; Hashimoto K et al., 2005; Bendikov I et al., 2007; Calcia M et al., 2012; Errico F et al., 2013; Nuzzo T et al., 2017). Excessive production/release of D-serine is implicated in acute and chronic degenerative disorders while abnormally low levels have been observed in patients affected by psychiatric disorders such as schizophrenia or bipolar disorders (Hashimoto K et al., 2003; Verrall L et al., 2007). In contrast to D-serine, little is known on the role of D-Asp in the brain. However, altered D-Asp levels have been proposed to contribute to NMDAR hypofunction found in brain of patients with schizophrenia (Balu DT, 2016; Coyle JT, 2012; Errico F et al., 2015; Nuzzo T et al., 2017). The brain levels of D-Asp and D-Ser are strictly regulated during development and may differ among brain areas. High levels of D-Asp have been found during fetal life with a rapid reduction after birth (Errico F et al., 2015).

D-Ser levels are more constant during life (Pollegioni et al., 2012) although it has been reported that they are high in cerebellum during early post-natal life and drop after 12-18 days in mice (Punzo et al., 2017; Miyoshi Y et al., 2012; Cuomo M et al., 2019). D-Ser and D-Asp levels are regulated at different levels (Errico F et al., 2006) but the enzymatic machinery that govern synthesis and degradation of these D-aminoacids have been partially characterized. It is known that D-aspartate oxydase (DDO) degrades D-Asp levels while D-amino acids oxydase (DAO) and serine racemase (SR) control synthesis (SR) and degradation (DAO) of D-Serine. Thus, considering the so fine mechanism controlling the spatio-temporal distribution of D-Asp and D-Ser levels, several evidence demonstrated that an imbalance in the levels or activities of DDO, DAO or SR enzymes might cause altered D-Asp and D-Ser metabolism and thus might be involved in the onset of schizophrenia (Yang HC et al., 2013; Jagannath V et al., 2018; Liu YL et al., 2016; Wood LS et al., 2007).

1.6 DNA methylation at genes encoding enzymes involved in D-amino acids metabolism.

There are several evidences showing the specific regional and cellular expression of DAO and DDO mRNA and protein in the human brain (Verrall et al., 2007; Habl et al., 2009; Ono et al., 2009). However, very few studies have addressed a role to DNA methylation in the transcriptional regulation of D-amino acid related genes. Jagannath et al. was the first group to report some information about DNA methylation specifically at DAO gene performing an *in-silico* analysis in the cerebellum and frontal cortex using GEO database. They identify a specific CpG site located in the exon 1 significantly more methylated in the cerebellum than in the frontal cortex. Regarding DDO gene, it has been demonstrated in some papers and in different experimental conditions that DNA methylation controls the increase in DDO transcription in a precise spatio-temporal manner (Punzo D et al., 2016; Florio E et al., 2017). By amplicon-bisulphite NGS, in whole brain of mice, eight CpG residues surrounding the transcription start site at DDO locus undergo to a decrease in methylation with a concomitant expression increase. Remarkably, the same and other gene regions at DDO locus have been analyzed in more detail analyzing five brain areas (prefrontal cortex, cortex, hippocampus, cerebellum, and striatum) from mice at post-natal day 30, in primary cortical neurons, microglia, oligodendrocytes, and astrocytes and in mouse embryonic stem cells. Taking advantage of a specific bioinformatic pipeline (Scala et al., 2016), the epialleles at DDO promoter region have been analyzed showing the presence of high rate of cell to cell heterogeneity (Florio E et al., 2017). In fact, neurons, oligodendrocytes, astrocytes, and microglial cells display distinct epiallele distribution at DDO promoter, indicating that epialleles could mark the cell-type identity. Taken together, these methylation studies emphasized the presence of well-orchestrated postnatal epigenetic events ensuring the proper control of DDO transcription (Florio E et al., 2017).

2. AIM OF THESIS

Dysregulation of D-amino acids system has been invoked as a contributor in the genesis and progression of schizophrenia and other neuropsychiatric and neurodegenerative conditions. D-serine (D-Ser) and D-aspartate (D-Asp) are present at substantial levels in the mammalian brain and are considered important neurotransmitter, having the ability to interact with NMDA receptor. For this reason, the brain levels of D-Asp and D-Ser must be strictly regulated during development and may differ among diverse brain areas. To ensure the correct and physiological brain levels of D-Ser and D-Asp, a specific enzymatic machinery intervene in their degradation: D-amino acid oxidase (DAO) enzyme, that degrades D-Ser and D-Aspartate oxidase (DDO), that instead metabolizes D-Asp. Since also the levels of DAO and DDO may be strictly orchestrated during development, I hypothesized that D-amino acids regulating genes may be subject to epigenetic control. Thus, the aim of my PhD project was to identify the existence of a physiological change in DNA methylation at these genes during developmental stages for a correct brain development. I provided a comprehensive and dynamic snapshot of epigenetic landscape at DAO and DDO genes along with mRNA expression and D-amino acids levels in schizophrenia disease and during brain development. I studied DNA methylation and demethylation dynamics at DAO and DDO genes in three mouse brain areas (Hippocampus, HIPP, Cerebellum, CB and Cortex, CX) at four different post-natal stages (Post-natal day 1, P1, Post-natal day 15, P15, Post-natal day 30, P30 and Post-natal day 60, P60). I also interrogated DNA methylation changes occurring in specific cell types, particularly in cerebellar astrocytes and neurons. Taking advantage of the very high coverage methylation analyses, I explored in depth the cell-to-cell methylation heterogeneity focusing on how much this phenomenon occur in a stochastic or a well-orchestrated fashion. In order to evaluate whether an organized distribution of the methylation profiles (epialleles) among the entire population of brain cells exists at D-amino

acid related genes in physiological and/or pathological conditions, I performed an ultra-deep methylation analysis (coverage: 200.000-300.000 reads/sample) of DAO and DDO promoters. I found for the first time consistent spatiotemporal modifications occurring at the DAO gene during neonatal development specifically in the cerebellum and within specific cell types (astrocytes). Moreover, I observed a dynamic demethylation event occurring especially at two specific CpG sites located just downstream of the transcription start site, measuring the level of 5'-hydroxymethylcytosine. This demethylation event was sufficient to strongly activate the DAO gene, ultimately promoting the complete physiological degradation of cerebellar D-serine few days after mouse birth. High amount of 5'-hydroxymethylcytosine, exclusively detected at relevant CpG sites, strongly evoked the occurrence of an active demethylation process. Once established the physiological distribution of DNA methylation at promoter region of these genes, I asked whether this epigenetic modification undergoes changes in specific pathological conditions. Thus, I analyzed DNA methylation at DAO and DDO promoters in post-mortem tissues (Dorsolateral Prefrontal Cortex, Hippocampus and Cerebellum) from patients with schizophrenia. Differential methylation and expression were detected across different brain regions, although no significant correlations were found with diagnosis. At DAO and DDO locus, I demonstrated that the analysis of epiallele distribution allowed me to detect differences in DNA methylation representing area-specific methylation signatures, which are likely not detectable with targeted or genome-wide classic methylation analyses. My results encourage the employment of epiallele approach to study DNA methylation since it may potentially give important information on cell identity and origin, functional state of a given gene and about the mechanisms underlying DNA methylation establishment, changes and, potentially, alterations of these processes in diseases.

3. MATERIAL AND METHODS

3.1 Collection of mouse brain tissue.

All experiments were performed on male animals. C57BL/ 6J mice were purchased from The Jackson Laboratory. Mice were housed in groups (n = 4 or 5) in standard cages (29 × 17.5 × 12.5 cm) at constant temperature (21–24 °C) and maintained on a 12/12 h light/dark cycle, with food and water ad libitum. All research was performed in accordance with the European directive 86/609/EEC governing animal welfare and protection, which is acknowledged by the Italian Legislative Decree no. 26 (March 14, 2014). Animal research protocols were also reviewed and approved by the local animal care committee at University of Naples “Federico II.” All efforts were made to minimize the animal’s suffering. Hippocampus, cortex, and cerebellum were collected from C57BL/6 J mice at different developmental stages, including the following time points: post-natal day (P) P1 (n=3), P15 (n=3), P30 (n=3), and P60 (n=3). All brain regions were dissected out within 20 s on an ice-cold surface. All tissue samples were pulverized in liquid nitrogen and stored at -80 °C for subsequent processing.

3.2 Isolation of neurons, astrocytes, and enriched microglia/oligodendrocyte/endothelial cells

Cerebral cortex and cerebellum were dissected from six to eight C57/BL6 mice at P1 and P15 and dissociated into a single-cell suspension using the Neural Tissue Dissociation Kit Postnatal Neurons (Milteny Biotec), according to the manufacturer’s protocol, with minor modifications [71, 72]. Briefly, after carefully removing the meninges, brain tissue was weighed and cut into small pieces in ice-cold Hank’s buffered salt solution (HBSS, Gibco). The minced tissue was then dissociated enzymatically in a solution of Enzyme Mix

1 for 25 min at 37 °C and then mechanically after adding Enzyme Mix 2. Finally, the sample was applied to a cell strainer, and the resulting single-cell suspension was centrifuged at 300×g for 10 min. Mouse astrocytes, neurons, and other non-neuronal cells were sequentially separated from the same brain samples with a magnetic activated cell sorting approach (MACS®). ACSA2-expressing astrocytes were enriched by positive selection using antibody-conjugated magnetic beads (Milteny Biotec). Neuronal cells were enriched by a negative depletion of non-neuronal cells using the Neuron Isolation Kit (Milteny Biotec). Briefly, up to 107 dissociated cells were resuspended in 80 µL of cold Dulbecco's phosphate- buffered saline containing 0.5% bovine serum albumin (DPBS-BSA buffer), incubated with 10 µL FcR Blocking Buffer for 10 min, and then with 10 µL ACSA-2 MicroBeads for 15 min, always at 4 °C. After washing, cells were centrifuged to remove excess beads from the solution. The pellet was suspended with 500 µL of DPBS-BSA buffer and the suspension was applied to the appropriate MACS column fitted in MACS Midi magnetic cell separator. The flow-through containing the unlabeled negative fraction was collected for subsequent cell separation. Following column removal from the magnetic separator, bound astrocytes were flushed out with 1 mL of DPBS-BSA, centrifuged, and the pellet stored at -80 °C for further analysis. Cell number in the negative fraction was determined and up to 107 dissociated cells were resuspended in 80 µL DPBS-BSA. Then, they were first incubated with 20 µL of Non-Neuronal Cell Biotin-Antibody Cocktail for 5 min and then with 20 µL di Anti-Biotin MicroBeads for 10 min, always at 4 °C. After resuspension in 500 µL buffer, the solution was eluted on MACS column. The flow-through containing the negative fraction of unlabeled neuronal cells was centrifuged and the pellet stored at -80 °C. Following column removal from the magnetic separator, bound non-neuronal cells (MOE fraction: mainly microglia, oligodendrocytes, and endothelial cells) were eluted in 1 mL buffer, centrifuged and stored. Cell identity and purity of astrocyte and neuronal fractions was confirmed in immunocytochemical experiments.

3.3 Human Tissue Samples Collection.

Dorsolateral prefrontal cortex and hippocampal samples from post-mortem brains were obtained from The Human Brain and Spinal Fluid Resource Center, Los Angeles Healthcare Center, Los Angeles, CA, USA (Brain Bank 1, BB1). Cerebellum tissue samples were obtained from the MRC London Neurodegenerative Disease Brain Bank of the Institute of Psychiatry, King's College London, UK (Brain Bank 2, BB2). All tissues were carried out under the regulations and licenses of the Human Tissue Authority and in accordance with the Human Tissue Act of 2004. Clinical diagnosis of SCZ was performed according to DSMIII-R criteria. Frozen tissues were pulverized in liquid nitrogen and stored at -80°C for subsequent processing.

3.4 DNA and RNA extraction protocols.

DNA from mouse and human tissues was prepared using DNeasy® Blood & Tissue Kit (Qiagen, Hilden, Germany), following the manufacturer's instructions. Total mRNAs were extracted using TRI REAGENT® (Invitrogen) solution, according to the manufacturer's instructions. DNA and RNA were quality checked by 260/280 absorbance ratio using NanoDrop 2000, (Thermo Scientific) and were quantified using respectively Qubit® 2.0 Fluorometer with the dsDNA broad range assay kit (Invitrogen, Q32850) and Nanodrop 2000 (RNA).

3.5 cDNA and Real Time experiments.

A total of 1 μg of total RNA of each sample was reverse-transcribed with Quanti Tect Reverse Transcription (QIAGEN) using oligo-dT and random primers according to the manufacturer's instructions. qRT-PCR amplifications

were performed using LightCycler 480 SYBR Green I Master (Roche Diagnostic) in a LightCycler480 Real Time thermocycler. The following protocol was used: 10 s for initial denaturation at 95 °C followed by 40 cycles consisting of 10 s at 94 °C for denaturation, 10 s at 60 °C for annealing, and 6 s for elongation at 72 °C temperature. The primers used for Real Time PCR both for mouse and for human are summarized in Table 1. β -actin and PP1A genes were used as housekeeping genes both in mouse and in human. Expression levels of all the transcripts analyzed were normalized to the geometric mean of the two housekeeping genes, β -actin and PP1A, and expressed as $2^{-\Delta Ct}$.

Gene	Species	Forward (5'-3')	Reverse (5'-3')
DAO	Mouse	TTTTCTCCCGACACCTGGC	TGAACGGGGTGAATCGATCT
DDO	Mouse	ACCACCAGTAATGTAGCGGC	GGTACCGGGTATCTGCAC
β -actin	Mouse	CTAAGGCCAACCGTGAAAAG	ACCAGAGGCATACAGGGACA
PP1A	Mouse	GTGGTCTTTGGGAAGGTGAA	TTACAGGACATTGCGAGCAG
DAO	Human	GGCATCTACAATTCCCCGTA	TGGAAGATGCCTCCAAGAGT
DDO	Human	GGTGTTCAATTTGGTATCAGGTTG	CTTTCGAAATCCCAGAACCA
β -actin	Human	TCCTCCCTGGAGAAGAGCTA	CGTGGATGCCACAGGACT
PP1A	Human	TTCATCTGCACTGCCAAGAC	CACTTTGCCAAACACCACAT

Table 1. Primers used for RealTime PCR for DAO and DDO genes in mouse and human

3.6 Bisulfite and oxidative bisulfite treatment

Bisulfite treatment was performed using EZ DNA Methylation Kit (Zymo Research). Genomic DNA (1 μ g) was converted with C/T conversion reagent and eluted in 50 μ l of H₂O following the manufacturer's instruction. To estimate the rate of bisulfite conversion, I used a spike-in control prepared by adding fully unmethylated M13mp18 double strand DNA (New England BioLabs) in 10 representative samples. After the library sequencing, I evaluated the conversion bisulfite of my experiments around 98- 99%. Oxidative bisulfite experiments for hydroxymethylcytosine detection at single nucleotide level were

performed using TrueMethyl oxBS module (Nugen, Tecan, California USA) following the manufacturer's instruction. Quality and amount (1 µg) of genomic DNA was evaluated by Nanodrop and Qubit instruments. DNA was first purified with magnetic beads and then treated with oxidant solution. Both bisulfite- and oxbisulfite-treated samples underwent to double amplification strategy to generate an amplicon library.

3.7 Amplicon Library preparation

To study the DNA methylation average and the epialleles distribution among different samples, I performed a double steps PCR strategy in order to generate a high quality of bisulfite amplicon library (Figure 4). After the bisulfite treatment, a first step of PCR was performed using primers generating amplicons of 300-400 bp. These primers contain overhang adapters sequences at each 5' end (FW: 5'-TCGTCGGCAGCGTCAGATGTGTATAAGAGACAG-3'; RV: 5'-GTCTCGTGGGCTCGGAGATGTGTATAAGAGACAG-3') that were recognized in the second step of PCR. Table 2 shows all primers sequences used to study DNA methylation at DAO and DDO promoters.

Gene	Species	Forward (5'-3')	Reverse (5'-3')	Amplicon	Tm Primers
DAO	Mouse	TagTTagagaagtTaggYtgYtYaYta	agattggtgaRRRaaaaaggagaga	+ 3/+ 365	52 °C
DDO	Mouse	gtgtgtttTgaggagtgaTaTtTa	aActtacctccattAAtccatAcc	- 63/- 468	52 °C
DAO	Human	aaggTTtgtTTaTaggggTtgaga	ccaActcaaaaAAtAcattctAccactc	-104/+221	54 °C
DDO	Human	aTTtaTaaatTagTtggagaaagTTTag	cctattcaAacactcccaactcc	-227/+171	52 °C

Table 2. Primers used for amplicon bisulfite PCR for DAO and DDO genes in mouse and human. Primers and amplification conditions used in the first PCR step for all genes in this study. The capital letters in the primer sequences indicate the original C or G. For all genes, the positions refer to the TSS

The first PCR conditions are: one cycle at 95°C for 2 min followed by 32 cycles at 95°C for 30 s, [primer Tm] for 40 s, 72°C for 50 s, followed by a final

extension step at 72°C for 6 min. Reactions were performed in 30 µl total volumes: 3 µl 10x reaction buffer, 0.6 µl of 10 mM dNTP mix, 0.9 µl of 5 µM forward and reverse primers, 3.6 µl MgCl₂ 25 mM, 2-4 µl bisulfite template DNA, 0.25 µl FastStart Taq, and H₂O up to a final volume of 30 µl. For both PCR steps, I used the FastStart High Fidelity PCR System (Roche). To eliminate the excess of primers I performed a first purification step using AMPure magnetic Beads (Beckman-Coulter, Brea, CA) with a ratio AMPure Beads/PCR products of 0.8. After this first purification step, I checked product sizes on 1.5% agarose gel. Then, I performed a second step of PCR, to add multiplexing indices and Illumina sequencing adapters. The condition of second PCR step were as follows: 50 µl total volume, 5 µl 10x reaction buffer, 1 µl dNTP mix, 5 µl forward and reverse Nextera XT primers (Illumina, San Diego, CA), 6 µl 25 mM MgCl₂, 5 µl of first PCR product, 0.4 µl FastStart Taq, and H₂O up to a final volume of 50 µl. Thermocycler settings were: one cycle at 95°C for 2 min followed by 8 cycles at 95°C 30 s, 55°C for 40 s, 72°C for 40 s, followed by a final extension step at 72°C for 5 min. As before, I repeated one AMPure Beads purification this time with a ratio Beads/PCR of 1.2. The quantification process and the check of amplicon quality were performed respectively using Qubit® 2.0 Fluorometer and Agilent 2100 Bioanalyzer DNA 1000 Kit (Agilent Technologies, Santa Clara, CA), according to the manufacturer's instructions. Finally, I prepared the amplicon bisulfite library. Each sample was diluted using 10 mM Tris pH 8.5 and brought to a final concentration of 4nM. Subsequently, 5µl of diluted DNA was mixed and the library were denatured with NaOH 0,2N. 5µl of 4nM pool was mixed with 5µl of NaOH 0,2 N with a final concentration of 1nM. Library was then diluted with a hybridization buffer (HT1). The library was diluted to a final concentration 8 pM in a final volume 600 µl. I used a Phix control libraries (Illumina) [15% (v/v)] to increase the diversity of base calling during sequencing. According to the Illumina protocols, I sequenced all different amplicon library with a V3 reagents kits on Illumina MiSeq system (Illumina,

San Diego, CA). Paired-end sequencing was carried out in 281 cycles per read (281 x 2). An average of 210,000 reads/sample were used for further analysis.

3.8 Sequence handling and bioinformatics analyses

The Illumina Miseq sequencer platform generates two FASTQ files for each sample. One file contains the sequences from forward primer and the other one with sequences from reverse primers. The first step to analyze the obtained sequences was evaluate the quality of each “read” using the FASTQC program. Then in order to acquire one unique FASTQ file, I used a PEAR tool (Zhang J et al., 2013) by selecting a minimum range of overlapping residues of 40 and a quality threshold a mean PHREAD score of at least. Then, FASTQ files were converted in FASTA format files using PRINSEQ tool (Schmieder R et al., 2011). The methylation status of each CpGs was evaluated using a pipeline software (Amplimethprofiler) that was developed in collaboration with a group of bioinformatics from my department. The pipeline is freely available at <https://sourceforge.net/projects/amplimethprofiler> (Scala G et al., 2016). This tool is specifically designed for deep targeted bisulfite amplicon sequencing of multiple genomic regions and provides functions to demultiplex, filter and extract methylation profiles directly from FASTA files. In my analysis, all kind of filters were taken into account (read length, percentage of similarity between the end of the read and the primer sequence, bisulfite efficiency, maximum percentage of ambiguously aligned CG sites, percentage of aligned read). Using these filters, all reads that did not match with expected length have been rejected. I used BLAST software (Camacho C et al., 2009) to align all reads to bisulfite reference of each gene in the analysis. As output, the pipeline returns: i) a summary and quality statistics file, containing information about the number of reads that pass filtering, the methylation percentage of each C in CpG sites, and the bisulfite efficiency for each C in non-CpG sites; ii) an alignment file where the bisulfite efficiency/read is calculated; iii) a CpG methylation profiles file,

3.9 Statistical analyses

All statistical analyses presented in my study were performed using Graphpad software (GraphPad Prism Software, Inc., La Jolla, CA, USA www.graphpad.com/guides/prism/7/statistics/index.htm). Every time I showed a methylation average data, I expressed the results as means \pm standard error. In all figures, the comparisons between 2 groups were performed using the unpaired Student t test, while multiple comparisons were made by 1-way ANOVA followed by Tukey post-hoc test. For all average methylation data, a P-value ≤ 0.05 was considered statistically significant. For what concern the statistical analysis of epialleles results, I decided to correlate the epialleles distribution within each stages group using a Pearson correlation test. For this kind of analysis, a P-value ≤ 0.001 was considered statistically significant. A principal component analysis (PCA) was performed on the abundance of each epialleles presents in the analyzed cell population. Beta diversity indicates the differences in epialleles assortment among groups and it assessed using “brain curtis distances”; this analysis is shown by principal coordinate analysis (PCoA) biplot that includes the impact of the epialleles driving the samples clustering.

4. RESULTS

4.1 The different applied methods to study DNA methylation

Amplicon bisulfite sequencing of a given genomic region enables us to determine with high precision whether each included CpG dinucleotide, in each single molecule, is methylated or unmethylated. Thus, the information that can be retrieved from high-coverage bisulfite sequencing are: (i) DNA methylation at each analyzed CpG site (here defined as "single CpG methylation"), calculated as the sum of how many times that CpG is found methylated in all the analyzed sequences for the specific sample. This analysis allowed me to understand whether some specific CpGs contributed more to the DNA methylation differences among the analyzed experimental conditions; (ii) average of DNA methylation considering all the analyzed CpG sites (here indicated as "average methylation"), calculated as the percentage of methylated cytosine in all the sequences for a specific sample; (iii) epiallele distribution analysis, that determine, with high precision, the combination of methylated and unmethylated CpG sites contained in the sequence. In this case, the methylation at each CpG site is considered in combination with the other CpG sites present in the amplicon. This latter analysis takes into account that CpG sites in an individual molecule may exist in a binary state (methylated, indicated with 1 or unmethylated, indicated with 0) and each individual DNA molecule, containing a certain number of CpGs, is a combination of these states defining an "epihaplotype". As an example, a region that includes 4 CpG sites may give origin to 16 possible combinations (2^4) that may be potentially found in a mixed population of cells (Figure 5). These different combinations will be here referred to as "epiallele"; the number of different exhibited epialleles provides a measure of the level of epipolymorphism (see Figure 5 for details and examples); (iv) epiallele classes analysis, that instead consider the number of methylated CpG sites/molecule, regardless the position of the CpG site. As an example, in a gene with 4 CpG sites, the number of epiallele classes are five: the 0-Meth class,

referred to the molecule that bear all the four CpGs in unmethylated status; the 1-Meth class, that included the sum of all the molecules containing only 1 methylated CpG (1000, 0100, 0010, 0001) unrelatedly to the position; the 2-Meth class, involving the sum of molecules bearing 2 methylated CpG sites and so on until the class with all CpGs in the methylated status. I applied all these DNA methylation analyses to each of the analyzed gene, in each analyzed brain area and developmental stage. Taking advantage of an ad-hoc bioinformatic pipeline, named "AmplimethProfiler" (Scala et al., 2016), I was able to investigate in one-step the single CpG methylation, the average methylation and epialleles distribution and evolution of the DAO and DDO genes in specific brain areas, during brain development and in schizophrenia. In the result section of my PhD thesis, I first discuss about average methylation and single CpG methylation analyses and then I focus on epiallele distribution analyses and epiallele classes analyses in all the investigated experimental conditions.

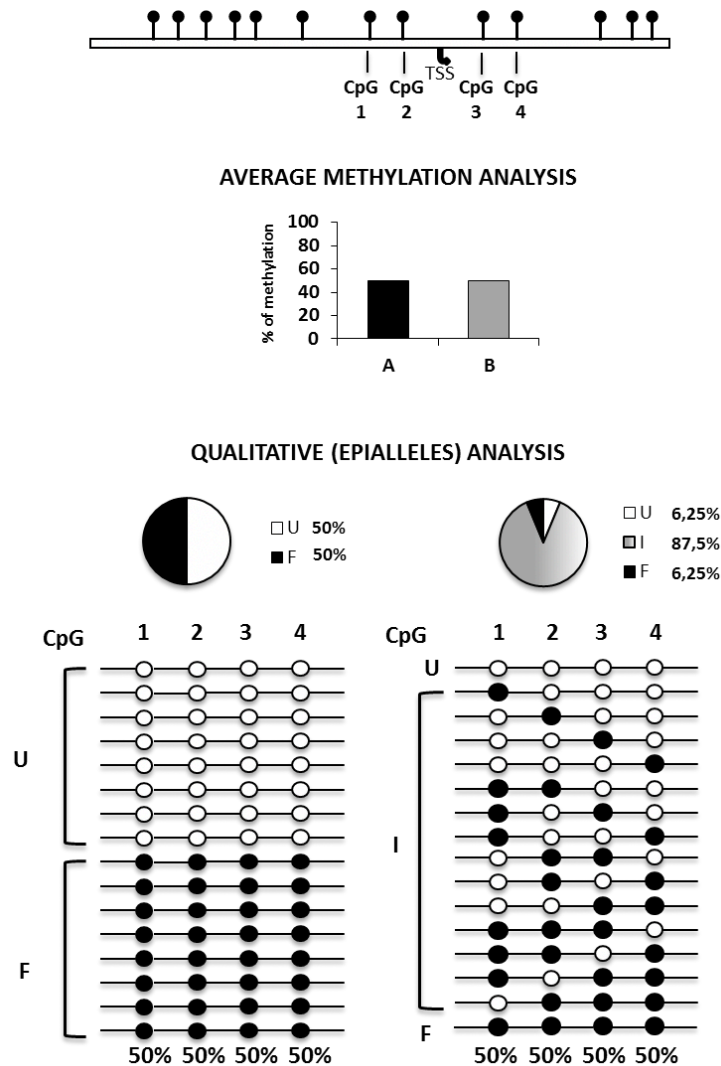


Figure 5. Schematic representation of epiallele concept. In the Figure is represented the analysis of a gene locus with 4 adjacent CpG sites. For this exemplificative gene it is reported an average methylation of 50%. This methylation degree may correspond to two completely different methylation scenarios. The first possibility is that, to get an average methylation of 50%, the sequencing return 50% of molecules with all 4 CpG sites in a completely un-methylated status and 50% of molecules with all 4 CpG sites in a completely methylated status. However, what generally happen (in non-imprinted loci) is that a quote of molecules is completely methylated and completely unmethylated but the majority of the sequences present a variable number of methylated CpG and unmethylated CpG. By this way, the average methylation is 50% but the distribution of methyl-C is not bimodal, and this information is not retrieved by the average methylation. TSS: transcription start site. The pie charts represent the percentage of fully unmethylated epialleles (U = white), fully methylated epialleles (F = black), and the 14 remaining possible methyl CpG combination or intermediate epialleles (I = gray gradient). (From Florio et al 2017)

4.2 Epigenetic landscape of genes involved in D-Ser and D-Asp metabolism during brain development in mice

Since it has been reported that DNA methylation regulates the expression of DDO gene leading to decreasing free D-Asp after birth (Punzo et al., 2016; Florio et al., 2017) during my PhD study I asked whether (i) DNA methylation controls the expression of DAO and DDO, indirectly controlling the levels of D-Ser and D-Asp; (ii) DNA methylation at DAO and DDO genes dynamically changes during brain development in mice; (iii) distribution of epialleles at DAO and DDO promoters is able to discriminate cell populations belonging to the different areas and stages. To answer to these questions, I involved in my studies cerebellum (CB), hippocampus (HIPPP) and cortex (CX) from mice at four different developmental stages (Post-natal day 1, P1; Post-natal day 15, P15; Post-natal day 30, P30; Post-natal day 60, P60). I performed all the above-mentioned methods to study DNA methylation, along with the measurement of D-Ser and D-Asp levels and mRNA expression analysis of DAO and DDO genes.

4.2.1 D-Asp and D-Ser levels in hippocampus, cortex and cerebellum of mice during development

As first step, I measured by HPLC the levels of D-Ser and D-Asp in the different analyzed brain areas (CX, HIPPP and CB) at P1, P15, P30 and P60 developmental stages. Considering that the levels of L- form of Asp and Ser in brain may impact on the amount of D-Ser and D-Asp, I expressed the values as the ratio of the amounts of the D- and total (D +L) forms of both Ser and Asp. I found that the D-Ser/total serine ratio significantly increased from P1 to P15 in both the hippocampus and cortex remaining high throughout the following postnatal phases (Figure 6a and b) Conversely, in the cerebellum, the D-Ser/total serine ratio underwent to a significant gradual reduction during the same postnatal development stages (Figure 6c). Regarding D-Asp, a strong reduction

of the D-Asp/total aspartate ratio was observed after P1 in the hippocampus, cortex and cerebellum and remained very low in all the following postnatal stages (Figure 6d, e and f).

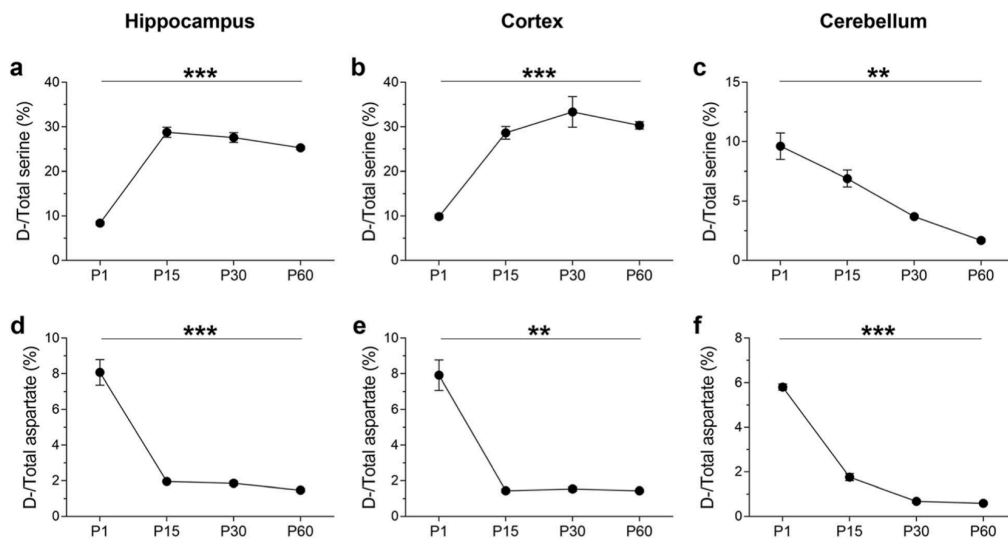


Figure 6. D-Ser and D-Asp contents in the mouse hippocampus, cortex, and cerebellum during ontogenesis. Average ratio of D-Ser/total Ser at different postnatal stages (P1, P15, P30, and P60) of C57BL/6 J mice in the a) hippocampus, b) cortex and c) cerebellum. Average ratio (expressed as %) of D-Asp/total Asp at different postnatal stages (P1, P15, P30, and P60) of C57BL/6 J mice in the hippocampus, cortex and cerebellum. The D- and L-forms of Asp and Ser were quantified by HPLC analysis. * $p < 0.05$, ** $p < 0.01$, *** $p < 0.0001$, compared with P1 (Fisher's post hoc). Data are expressed as the mean \pm SEM. (From Cuomo et al., Clinical Epigenetics, 2019)

4.2.2 *DAO and DDO gene structures in mice*

Because the DNA methylation effects on gene expression are strictly dependent on the analyzed gene region, I first identified the promoter region of the D-amino acid related genes and studied the CpG conformation of each promoter. The DAO promoter region is a CpG poor presenting a very few numbers of CpG sites surrounding the transcriptional start site (TSS, indicated by the black arrow in Figure 7 and considered as +1). I choose to focus on a region of 389 nucleotides of the DAO promoter that contains four CpG sites (+7; +101; +217; +334), all of which are located downstream of the TSS. These characteristics make DAO gene an excellent candidate to study epiallele distribution. In fact, considering the 4 CpGs enclosed in the analyzed region, the possible epiallele combinations are 2^4 , and so 16. A so limited number of epialleles ensured a high sequences coverage for each epiallele and make me confident about their distribution in all analyzed brain areas at all different developmental stages. In order to draw a complete snapshot of DNA methylation distribution on DAO gene, I investigated DNA methylation at DAO promoter also in the region upstream the TSS (data not shown). For DDO, I decided to analyze a region previously reported to be regulated by DNA methylation (Florio et al., 2017). This region of 405 bp carries six CpG sites and is located upstream of the TSS. As shown in Figure 7, the number of all CpG sites is referred to the TSS, indicated with +1.

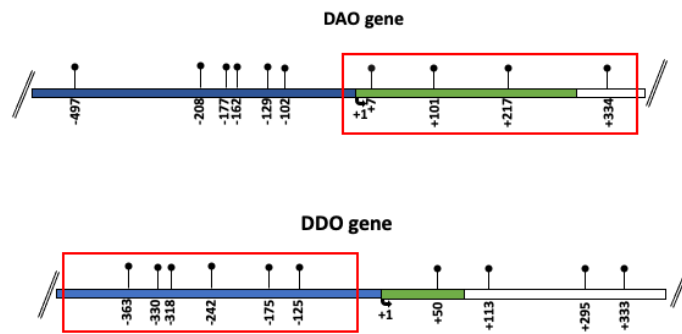


Figure 7. DAO and DDO promoter regions showing the position of the analyzed CpGs. The numbers of the CpG sites refer to the putative transcriptional start site (TSS), indicated with + 1. Blue box indicates the putative upstream regulatory region; green box indicates the first exon; and white box indicates the first intron. Red rectangles specify the amplicon used for bisulfite sequencing.

4.2.3 DNA methylation and mRNA expression levels at DAO promoter in Hippocampus, Cerebellum and Cortex during brain development

I analyzed the average methylation level at the DAO promoter in Hippocampus (HIPP), Cortex (CX) and Cerebellum (CB) at four developmental stages (Post-Natal day 1, P1, P15, P30 and P60). I first evaluated the average methylation levels at P1, P15, P30, and P60 in all analyzed brain regions (Figure 8A). In HIPP and CX, I found high level of average methylation (approximately 75%) that remained stable during the different stages. Conversely, striking and significant differences in the average DNA methylation were observed in CB where the higher degree of methylation was observed at postnatal day 1 ($71.5\% \pm 0.03$) and drastically reduced at P15 ($43.5\% \pm 0.02$), P30 ($44.8\% \pm 0.004$), and P60 ($53.1\% \pm 0.003$). These data strongly correlated with mRNA expression levels in HIPP, CX, and CB during brain development (Figure 8B). Very low DAO expression levels were observed in HIPP and CX in all developmental stages, while in CB I found a significant (one-way ANOVA; $p \leq 0.001$) increase in DAO mRNA expression during ontogenesis (Figure 8B). I then evaluated the methylation average at single CpG resolution during brain development in HIPP, CX, and CB (Figure 8C). In HIPP and CX, no differences in single CpG methylation were found at each developmental stage. In contrast, in CB brain region, I observed a marked significant decrease in methylation level especially at CpG +7 and +101 sites from P1 to P15 (from 52.8 ± 0.06 to $8.2 \pm 0.02\%$) remaining low at P30 and P60. A transitory decrease of methylation at CpG +217 from P1 to P15 was observed that increased again (reaching above 80% of methylation average) at P30 and P60. Conversely, CpG + 334 exhibited high and constant levels of methylation also in CB area.

In order to evaluate whether this demethylation phenomenon regarded specifically the CpG sites surrounding the TSS promoter or involved other CpG sites located upstream of the TSS, I analyzed also a region ($-234/+137$ nts, data not shown) that included both five additional CpG sites located upstream (-208 , -177 , -162 , -129 , and -102) and the abovementioned + 7 and + 101 sites in a

single amplicon. I found that all the CpG sites located upstream the TSS showed a low degree of methylation at each of the analyzed developmental stage and thus the methylation decrease during cerebellum development was essentially limited to the CpG +7 and CpG + 101 (data not shown).

Taking together all the methylation analyses and the mRNA expression data, the selective reduction of DNA methylation observed in the cerebellum from P1 to P15 at two CpG sites (+ 7 and + 101 sites) might be functionally associated with the robust activation of the DAO gene during that temporal window and ultimately with the dramatic reduction of the D-Ser concentration identified in the mouse cerebellum at P30.

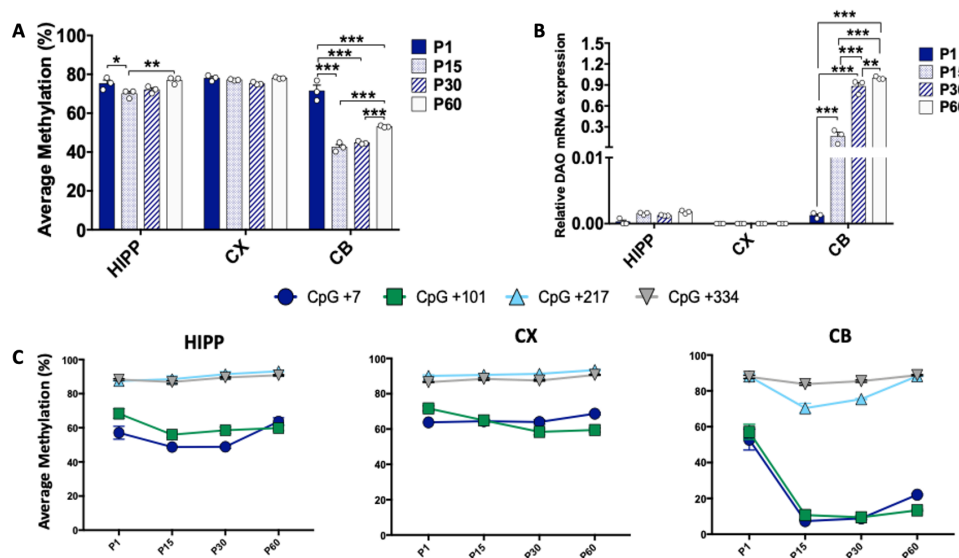


Figure 8. Methylation analyses at DAO gene. A) HIPP, CX and CB average methylation is represented at the P1, P15, P30, and P60 developmental stages (n = 3 mice/stage). Comparisons between developmental stages in each area were performed using one-way ANOVA followed by Tukey's multiple comparison post-hoc test. * $p \leq 0.001$. B) mRNA expression levels for each analyzed brain area during brain development is reported and DAO mRNA expression was normalized to the mean of two housekeeping genes and is expressed as $2^{-\Delta Ct}$ values, * $p \leq 0.001$ (one-way ANOVA followed by Tukey's multiple comparison post-hoc test). C) Average methylation at single CpG resolution in HIPP, CX, and CB during ontogenesis is shown. (From Cuomo et al., Clinical Epigenetics, 2019)

4.2.4 Analysis of 5-mCpG and 5-hmCpG dynamics at DAO promoter region

During brain development, the number and the type of cells composing a specific brain area radically change. Thus, the demethylation phenomenon that I observed at DAO promoter region may be the result of an increase in number of cells that bear a demethylated DAO promoter already at P1, causing a passive demethylation mechanism. Nevertheless, DAO promoter region may be exposed to an active demethylation process, mediated by TET family enzymes. Bisulfite analysis performed in this study is not able to distinguish between 5-mC and 5-hmC. Thus, in order to elucidate whether DAO gene undergoes to an active or passive demethylation process during cerebellum development, I performed an oxidative bisulfite sequencing (Booth MJ et al., 2013) measuring the levels of 5-hmC at the same DAO region analyzed before in CB at P1 and P15. This technique involves the use of an oxidizing agent capable of removing hydroxymethyl modification so that after bisulfite the cytosine is read as thymine. Thus, the levels of 5-hmC levels was calculated by subtracting the average methylation obtained with bisulfite sequencing and the average methylation values obtained after treatment with oxidant reagent and bisulfite. Results, shown in Figure 9, revealed the presence of high amount of hydroxymethylation at CpG + 7 and CpG + 101 at P1 indicating that these sites were actively demethylated likely by TETs protein (Figure 9). Also CpG + 217 exhibited high levels of 5-hmC at P1 but at this specific site the levels of 5-mC increased at P15. These findings likely suggest that the TET enzymes activity predominated on the activity of DNMTs specifically at + 7 and + 101 CpGs. Strikingly, at the + 334 CpG, 5-methylcytosine was very stable and was not exposed either to hydroxymethylation or to demethylation phenomena over time.

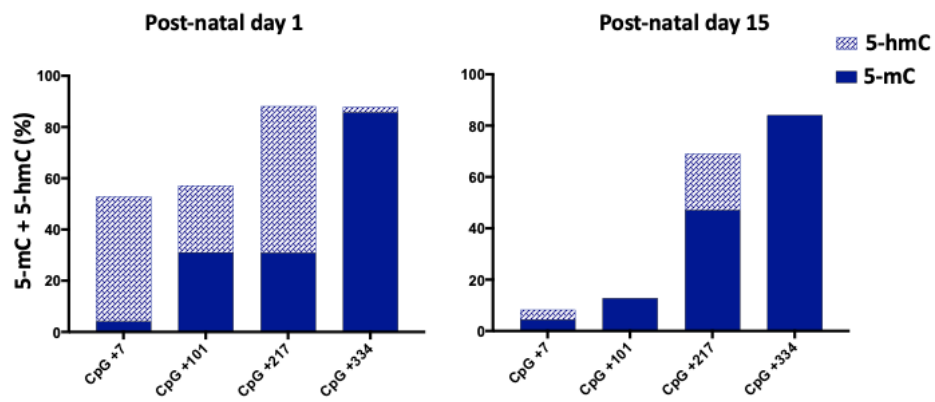


Figure 9. Comparison of 5-mCpG and 5-hmCpG levels at single-CpG resolution of DAO promoter in CB area. Levels of methylation (blue) and hydroxymethylation (white line pattern) at DAO single CpG sites from P1 to P15 stages. For each time point, results are indicated as the mean of n=3 mice. (From Cuomo et al., Clinical Epigenetics, 2019)

4.2.5 DNA methylation dynamics in cerebellar astrocytes and neurons during the P1-P15 temporal window

Considering the high cellular heterogeneity of cerebellum tissue, I questioned whether some specific type of cell composing cerebellum present a major demethylation effect. Thus, I isolated astrocytes, neurons and a fraction containing microglia, oligodendrocytes, and endothelial cells (MOE fraction) from cerebellum tissues at the P1 and P15 time points and I analyzed DAO promoter methylation (Figure 10). The results showed that the decrease in methylation levels during P1 to P15 transition mainly occurred in astrocytes compared to neurons and other cell types (Figure 10). Even though these results do not exclude the passive demethylation process (at these postnatal stages astrocytes are likely active proliferating cells (Farhy-Tselnicker I et al., 2018)) together with oxidative bisulfite sequencing analysis, it is very likely that an active demethylation event is occurring at + 7 and + 101 CpGs and specifically in cerebellar astrocytes from P1 to P15.

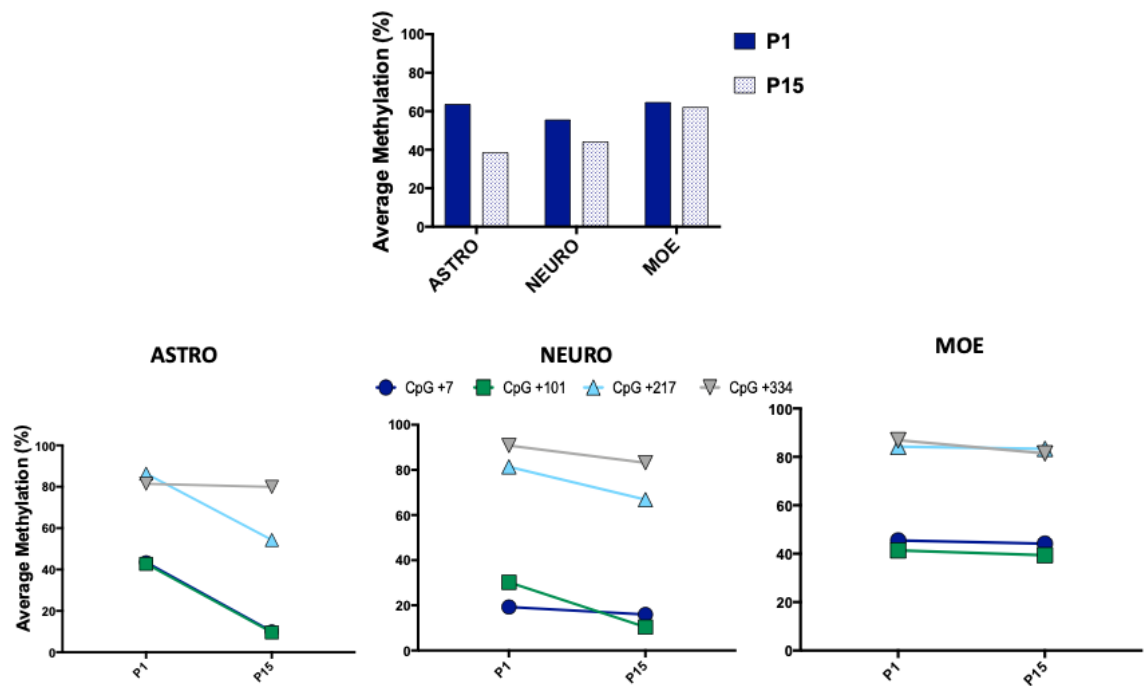


Figure 10. DAO methylation levels in different cell types at the P1 and P15 stages in cerebellum. On the top, DAO average methylation (%) in astrocytes, neurons, and a fraction containing microglia, oligodendrocytes, and endothelial cells (MOE fraction) at postnatal days 1 and 15. On the bottom, DAO single-CpG methylation average in astrocytes, neurons and MOE fraction during the transition from P1 to P15. (From Cuomo et al., Clinical Epigenetics, 2019)

4.2.6 DNA methylation and mRNA expression of the DDO gene in different brain areas at different developmental stages

It has been previously reported that DDO gene in whole brain increase in mRNA expression after birth with a concomitant reduction of cerebral D-Asp levels (Florio et al., 2016). It has been also elucidated that DNA methylation controls DDO mRNA expression and that at early post-natal development DDO promoter region undergoes to a decrease in methylation. Thus, I investigated whether methylation decrease at DDO locus occurs in specific brain areas and post-natal stages. As at DAO gene, I analyzed the DNA methylation state and mRNA expression of the DDO gene in HIPP, CX, and CB at P1, P15, P30, and P60 (Figure 11). In CX region, I did not observe any differences either at average methylation nor at single CpG resolution during development (Figure 11A and B), although I observed a slight temporal increase in mRNA expression (Figure 11C). Conversely, in HIPP area I found a significant decrease (one-way ANOVA; $p = 0.001$) in average methylation from P1 to P60 (Figure 11A) and this demethylation regarded all the analyzed CpG sites, especially from P1 to P15 (Figure 11B). In accordance with decrease in DNA methylation, I observed a significant increase (one-way ANOVA; $p \leq 0.001$) of DDO mRNA levels during ontogenesis (Figure 11C). A decrease of DDO DNA methylation was observed also in CB from P1 to P15 that then slightly increased at P30 and P60 (Figure 11A). Accordingly, DDO mRNA expression significantly (one-way ANOVA; $p \leq 0.001$) increased over time in the cerebellum area (Figure 11B). Very interestingly, at single CpG level, I observed that methylation levels at all six CpG sites tended to decrease from the P1 to P15 stages, remaining then consistently low only at the -125 and -175 CpG sites (Figure 11C). Conversely, a minor increase in methylation at the other CpG sites (Figure 11C) was observed, possibly explaining the higher average methylation levels observed from developmental stages P15 to P60 (Figure 11A).

Overall, these data identified a key role for the methylation at the -125 and -175 CpG sites in the control of DDO expression during brain development.

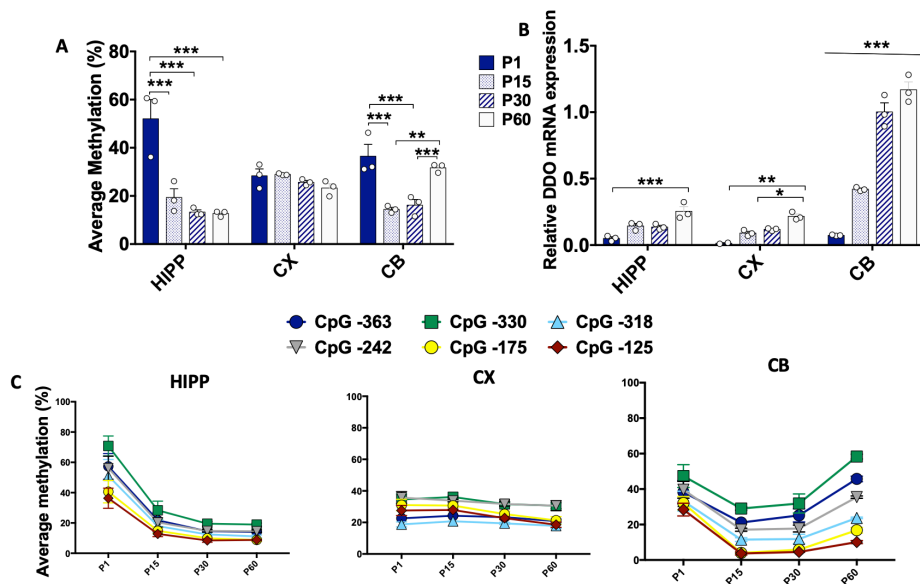


Figure 11. DNA methylation and mRNA expression at the DDO promoter region. A) HIPP, CX and CB average methylation at DDO promoter is represented at the P1, P15, P30, and P60 developmental stages (n = 3 mice/stage). Comparisons between developmental stages in each area were performed using one-way ANOVA followed by Tukey's multiple comparison post-hoc test. * $p \leq 0.001$. B) mRNA expression levels for each analyzed brain area during brain development is reported and DDO mRNA expression was normalized to the mean of two housekeeping genes and is expressed as $2^{-\Delta Ct}$ values, * $p \leq 0.001$ (one-way ANOVA followed by Tukey's multiple comparison post-hoc test). C) Average methylation at single CpG resolution at DDO gene in HIPP, CX, and CB during ontogenesis is shown. (From Cuomo et al., Clinical Epigenetics, 2019)

4.3 DNA methylation and mRNA expression scenario of DAO and DDO genes in post-mortem tissues from patients with schizophrenia

D-Asp and D-Ser levels are believed to play a role in NMDA-related function, being agonist and co-agonist of NMDA receptor, respectively. Considering the epigenetic regulation of DAO and DDO genes found in mice during development, I hypothesized that epigenetic profiling might drive the correct spatio-temporal modulation of these genes also in human brain. Consequently, an alteration in DNA methylation controlling the expression at these genes could be linked to human brain disorders, including schizophrenia. Thus, I performed an ultra-deep analysis of DNA methylation along with expression profiles DAO and DDO genes in post-mortem hippocampus (HIP), dorso-lateral prefrontal cortex (DLPFC) and cerebellum (CB) from non-psychiatric subjects (CTRL) and patients with schizophrenia (SCZ). For this study, I used HIP and DLPFC from 20 non-psychiatric control and 20 patients with schizophrenia from the brain bank "The Human Brain and Spinal Fluid Resource Center" in Los Angeles Healthcare Center, Los Angeles, CA, USA while CB tissues were obtained from 10 non-psychiatric control and 9 patients with schizophrenia derived from another bank (MRC London Neurodegenerative Disease Brain Bank of the Institute of Psychiatry, King's College London, UK). As in previous experiments in mice, I also performed epiallele classes and distribution analyses in order to finely identify cell to cell methylation differences in specific brain areas and to evaluate whether these ultra-deep methylation profiles may distinguish brain areas within each individual and/or be associated to schizophrenia diagnosis.

4.3.1 DAO and DDO gene structures in human

As in mouse, I evaluated the promoter regions of DAO and DDO genes in humans. The majority of CpG sites at DAO gene are located in proximity of the TSS. I choose to analyze a region of about 400 nt containing 10 CpG sites (-40; -30; -26; +11; +30; +74; +82; +105; +153 and +193) surrounding the transcriptional start site (TSS). Also the DDO promoter region presents a cluster of CpG sites in the closeness of TSS and in this case, I analyzed a region with 7n CpG sites encompassing the TSS.

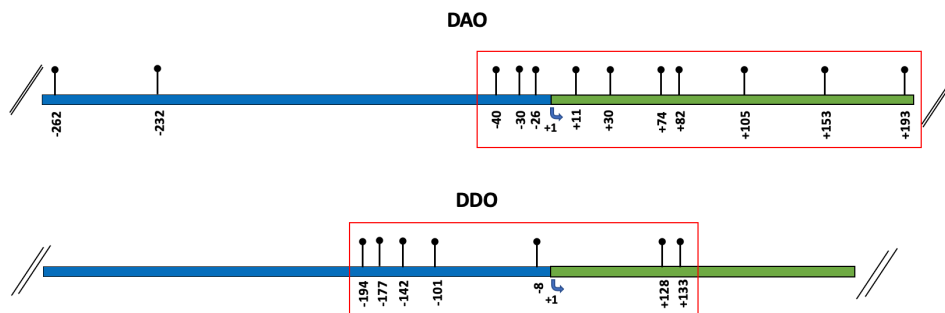


Figure 12. DAO and DDO promoter regions in humans showing the position of the analyzed CpGs. The numbers of the CpG sites refer to the putative transcriptional start site (TSS), indicated with + 1. Blue box indicates the putative upstream regulatory region; green box indicates the first exon. Red rectangles specify the amplicon used for bisulfite sequencing.

4.3.2 Analysis of DNA methylation and mRNA expression at DAO gene promoter in non-psychiatric subjects and patients with schizophrenia.

Using high-coverage targeted bisulfite sequencing, I analyzed DNA methylation status of DAO gene in HIPPC, DLPFC and CB. I interrogated DNA methylation at DAO promoter in a region containing 10 CpG sites (-40; -30; -26; +11; +30; +74; +82; +105; +153 and +193) surrounding the DAO transcriptional start site (TSS) (Figure 12). No differences in average methylation and single CpG methylation levels were found comparing CTRL and SCZ groups in all analyzed brain areas with the exception of CB area, where a slight decrease at +11, +30, +82, +105 and +153 CpG sites were found in schizophrenia-affected patients with respect to non-psychiatric controls (Figure 13A and B). I then evaluated the DAO mRNA expression and I found that in both HIPPC and DLPFC, regardless of the diagnosis, DAO mRNA levels were very low. Conversely, higher DAO mRNA levels were found in the CB, without significant differences between CTRL and SCZ subjects (Figure 13C).

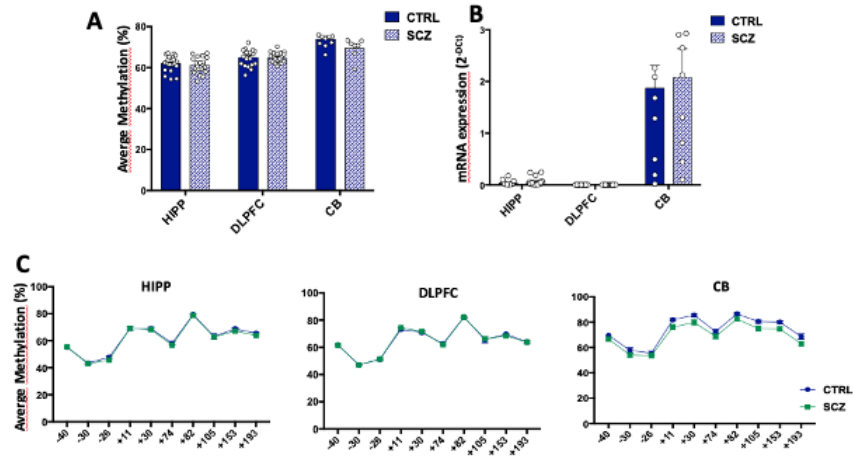


Figure 13. DAO promoter methylation and mRNA expression in patients with schizophrenia and non-psychiatric controls in different post-mortem tissues A) HIPP, DLPFC and CB average methylation at DAO promoter is represented in CTRL and SCZ groups. White circle indicates the patients and controls. B) DAO mRNA expression levels for each analyzed brain area in CTRL and SCZ groups is reported and expressed as $2^{-\Delta\text{Ct}}$ C) Average methylation at single CpG resolution in HIPP, DLPFC, and CB in CTRL and SCZ groups. All data are shown as the mean \pm standard error (SEM). (From Keller, Punzo, Cuomo et al., Scientific Report, 2018)

4.3.3 DDO promoter methylation and mRNA expression in non-psychiatric subjects and patients with schizophrenia.

I analyzed average methylation in HIPP, DLPFC and CB (Figure 14) at DDO promoter gene. Overall, HIPP and DLPFC brain regions presented a higher average methylation compared to CB area (Figure 14A) and in CB and in HIPP no significant differences were found between schizophrenia and control groups (Figure 14A). Conversely, I found a slight but significant DDO methylation increase in the HIPP of patients with schizophrenia, compared to control group (Figure 14A). However, these data did not correlate with mRNA expression levels of DDO gene, low DDO mRNA expression in CB and DLPFC was detected, with no significant differences between patients and controls, and higher levels in HIPP without differences between diagnosis (Figure 14B). At single CpG levels, I found a slight but not significant increase in methylation levels in the HIPP of SCZ patients compared to CTRL subjects at all analyzed CpG sites. Also in DLPFC and CB, I found no significant difference between diagnoses (Figure 14C).

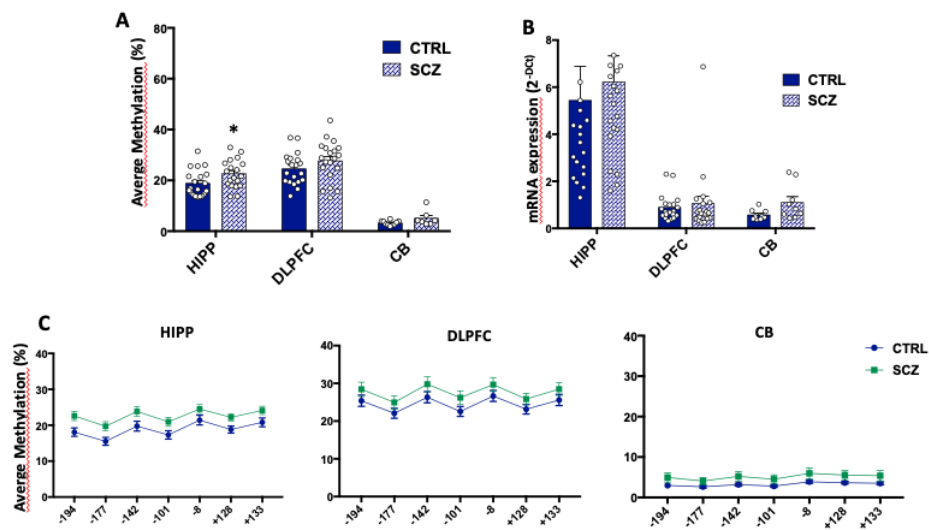


Figure 14. Methylation and expression studies of the DDO gene. A) DDO promoter methylation and mRNA expression in patients with schizophrenia and non-psychiatric controls in different post-mortem tissues A) HIPP, DLPFC and CB average methylation at DDO promoter is represented in CTRL and SCZ groups. White circle indicates the patients and controls. B) DDO mRNA expression levels for each analyzed brain area in CTRL and SCZ groups is reported and expressed as $2^{-\Delta\text{Ct}}$ C) Average methylation at single CpG resolution in HIPP, DLPFC, and CB in CTRL and SCZ groups. All data are shown as the mean \pm standard error (SEM). (From Keller, Punzo, Cuomo et al., Scientific Report, 2018)

4.4 Epiallele distribution analysis and epiallele classes analysis at DAO and DDO promoters in mice during brain development and in patients with schizophrenia

Recently, a new way (epialleles analysis) to study the DNA methylation has been demonstrated (Florio et al., 2016). This method may reveal some fine changes in methylation status of certain genes indicative of cell-to-cell heterogeneity in terms of methylation. Moreover, epialleles allow one to detect single molecule methylation profiles and may be considered a proxy of single cell analysis. Thus, tracking epiallele profiles may help “to identify barcodes” to get insight into mechanisms underlying DNA methylation establishment, changes and, potentially, alterations of these processes in neurodevelopmental diseases that may be not revealed by conventional, either gene specific or genome-wide, average methylation analyses. For these reasons, I applied epiallele distribution and epiallele classes analyses at DAO and DDO locus in all experimental conditions of my PhD work.

4.4.1 Epiallele distribution analysis in different brain areas during brain development at DAO gene

In order to investigate whether epiallele distribution at the DAO gene locus is able to distinguish specific brain areas and/or developmental stages, I performed epiallele distribution analysis in HIPP, CX and CB at all analyzed time points (Figure 15). As said above, this method, that requires a large number of sequences reads per sample, allowed me to quantitatively and qualitatively track the arrangements of methyl-CpG combination, defined epialleles, at a specific locus at single-molecule level. Sequences obtained by ultradeep bisulfite sequencing were processed via the ampliMethProfiler pipeline (<https://sourceforge.net/projects/amplimethprofiler>) (Scala et al., 2016). This "ad-hoc" pipeline generated a BIOM format table containing the amount of DAO epialleles in all samples. Different proportions of all the possible epialleles (16)

were found in each brain area and developmental stage. In order to verify if the epiallele distribution at DAO locus was able to discriminate among the different brain region and developmental time points, I performed principal coordinate analysis (PCoA) (Figure 15). Surprisingly, I found that the epiallele distribution in HIPP and CX showed strong grouping of the diverse developmental points, although the average methylation in HIPP and CX did not change during ontogenesis. Interestingly, in CB each developmental stage clearly grouped and, even though this phenomenon was quite expected from the average methylation differences, also P30 and P60, that showed a very similar average methylation, were distinctly separated in the PCoA plot. I then asked whether epiallele distribution analysis is able to discriminate also the different analyzed brain areas. I performed hierarchical clustering by combining HIPP, CX and CB and all developmental stages. As expected by average methylation analysis, CB area distinctly clustered away from HIPP and CX, denoting a different epiallele distribution. Interestingly, the cerebellum area at early development (P1) presented a shared epiallelic patterns with HIPP and CX, whereas at later stages, the epiallelic profiles moved away in a distinct manner.

These results shed in light the high power of epiallele distribution analysis in unravel information that average methylation or single CpG methylation might hide. Moreover, epiallele distribution analysis showed a non-stochastic and well-orchestrated DNA methylation remodeling that was influenced by the specific brain areas and developmental time points.

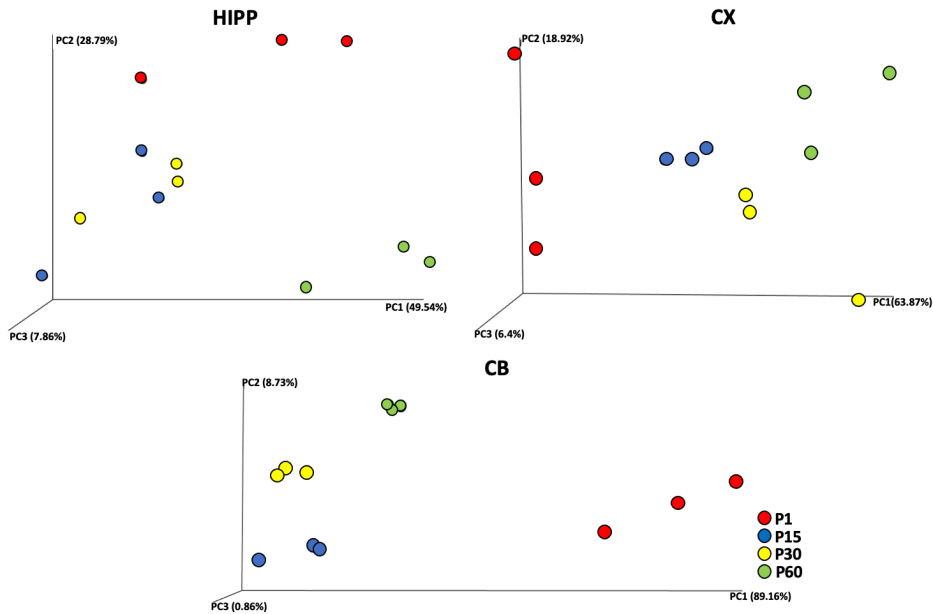


Figure 15. Epialleles distribution analysis of the mouse DAO gene during brain development in HIPP, CX, and CB. Principal coordinate analysis (PCoA) plots show the distribution of the different time points P1 (red), P15 (blue), P30 (yellow), and P60 (green) according to their epiallele composition. The plots are derived from the qualitative and quantitative influence of each of the 16 epialleles discriminating the different time points P1 (red), P15 (blue), P30 (yellow), and P60 (green) in each analyzed brain area. Adjacent samples share similar epiallelic composition.

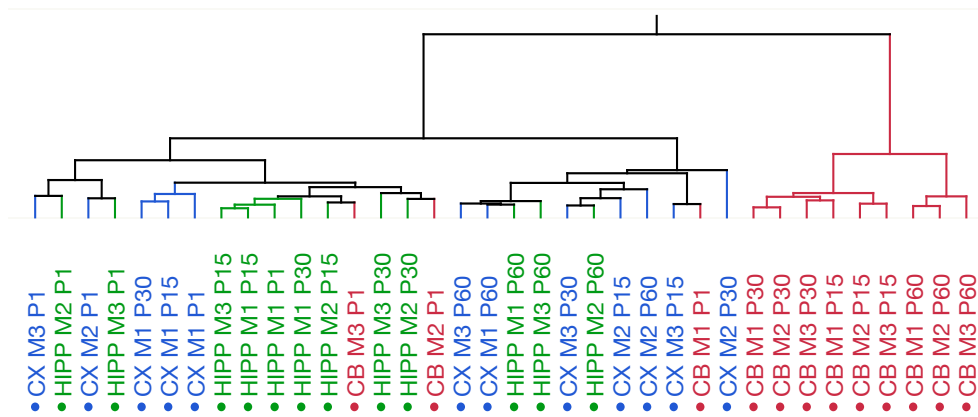


Figure 16. Hierarchical cluster of brain region differences based on the epiallelic composition at mouse DAO gene including all developmental stages.

4.4.2 Spatio-temporal distribution of epialleles at DDO gene during mouse brain development.

Then, I performed DDO epiallele analysis of specific areas over time (Figure 17). As expected from average methylation (at P1, the average methylation is significantly higher compared to P15, P30 and P60; Figure 11A), epiallele distribution in HIPP showed a clear clustering of P1 away from the other developmental stages that instead grouped together (Figure 17). Moreover, in CX, DDO epiallele profiles were not able to distinguish the developmental stages. Also for DDO, epiallele distribution analysis showed greater results in CB, where all the time points differently clustered, with the exception of P15 and P30. However, P1 and P60, although sharing a very similar average methylation, grouped separately one which other and from P15 and P30, likely indicating that during brain development a mechanism of methylation dynamicity characterized DDO gene promoter (Figure 17). Finally, I performed hierarchical cluster analysis (HCA) pooling together the epialleles of all analyzed developmental stages and brain areas (Figure 18). By this analysis, I found that especially CX brain area clearly clustered with respect to CB and HIPP. Nevertheless, also HIPP and CB presented a selective epiallele profile that made these tissues distinguishable, with the exception of P1 in HIPP (Figure 18).

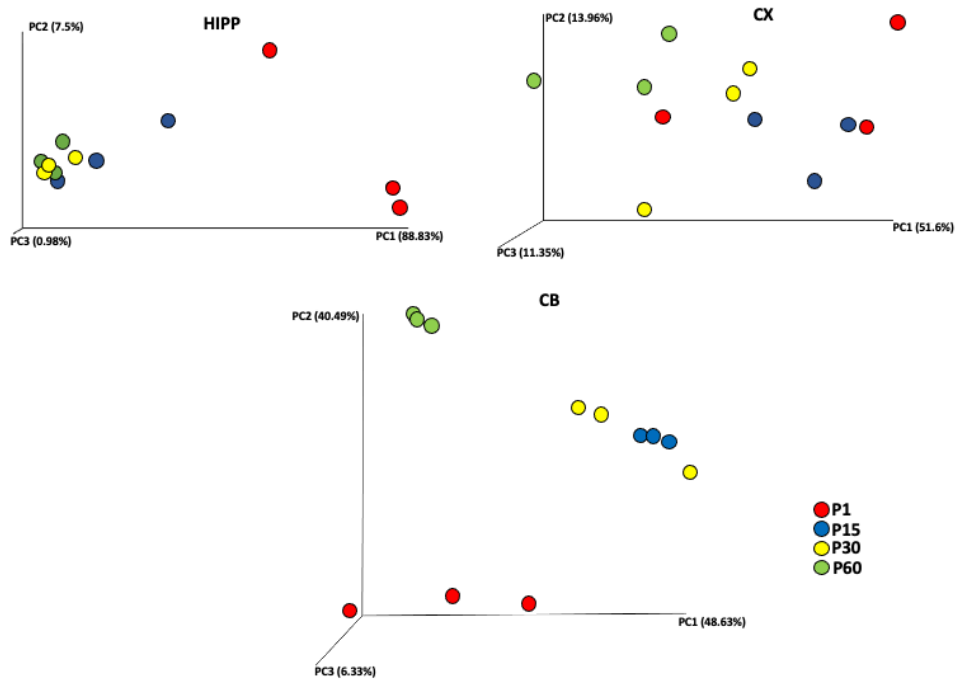


Figure 17. Epialleles distribution analysis of the mouse DDO gene during brain development in HIPP, CX, and CB. Principal coordinate analysis (PCoA) plots show the distribution of the different time points P1 (red), P15 (blue), P30 (yellow), and P60 (green) according to their epiallele composition. The plots are derived from the qualitative and quantitative influence of each of the 16 epialleles discriminating the different time points P1 (red), P15 (blue), P30 (yellow), and P60 (green) in each analyzed brain area. Adjacent samples share similar epiallelic composition.

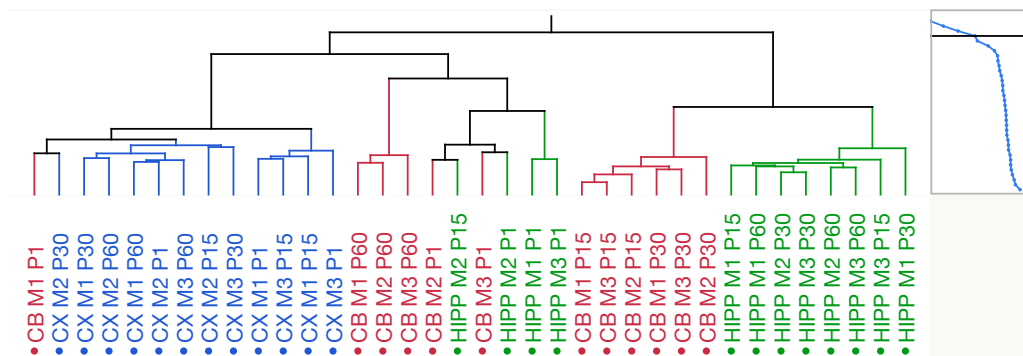


Figure 18. Hierarchical cluster of brain region differences based on the mouse DDO epiallelic composition is shown, including all developmental stages.

4.4.3 Single molecules DAO methylation analyses in non-psychiatric subjects and patients with schizophrenia.

I then applied epialleles distribution analysis to evaluate single molecule differences at DAO promoter methylation in CTRL and SCZ samples. The DAO analyzed region contains 10 CpG sites (Figure 12) and the number of possible epiallele combinations is 1024. For this reason, I decided to perform first epiallele classes analysis, taking into account all the epialleles bearing the same number of methylated CpG sites regardless their position (Figure 19A). I found no significant differences between CTRL and SCZ groups. Nevertheless, the different analyzed brain areas showed remarkable differences in the epiallele classes distribution, despite HIPP, DLPFC and CB did not present significant differences in average methylation. Especially in CB, a peculiar profile in term of methylation classes distinguished this brain area from the others. In addition, a statistically significant difference between HIPP and DLPFC ($p = 0.01$) was identified. This area-specific epiallele classes distribution may likely mirror the dissimilar cell type composition of the analyzed brain areas and/or the functional state of the gene in individual cells composing the different tissues. Even though no great differences were found comparing diagnosis, 57.1% of SCZ patients in CB displayed a percentage of the 0-methylated class $\geq 10\%$, while only 10% of non-psychiatric controls presented the percentage $\geq 10\%$ (Figure 19A). Considering that the 0-Meth class correspond to the molecules with no CpG in methylated status, these molecules should correspond to the ones expressing DAO gene. Thus, this may possibly indicate a greater number of cells expressing DAO gene in CB of SCZ compared to CTRL groups. Next, I performed epialleles distribution analysis including all brain areas and SCZ and CTRL groups. The Principal coordinate analysis (PcoA) plot (Fig. 2C), based on the epiallelic composition similarities among all individual samples, displayed a significant and striking clustering of HIPP and DLPFC against CB areas (Figure 19B).

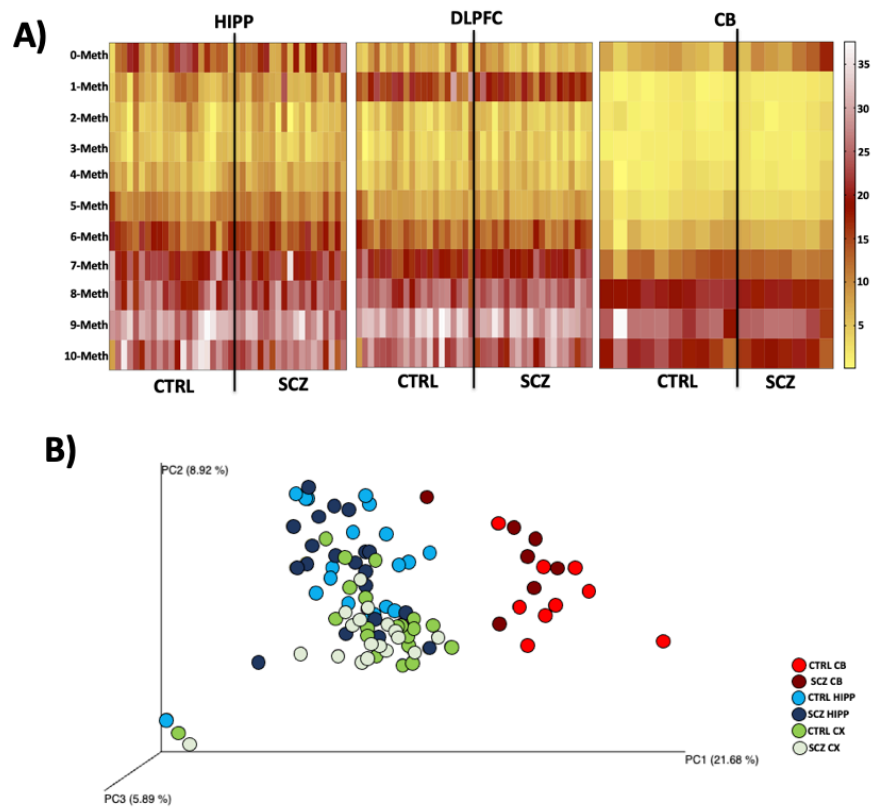


Figure 19. Epiallele classes and distribution analyses at human DAO gene. (A) Heatmaps show the abundance of all the different epiallele classes (from 0 to 10 methyl-cytosine per molecule) in each sample and in all analyzed brain regions (hippocampus = HIPP; dorsolateral prefrontal cortex = DLPFC; cerebellum = CB). The color gradient from yellow to white indicates the percentage of each epiallelic class. (B) Epialleles distribution analysis of the human DAO gene, taking in consideration all brain region and both groups, is shown in the principal coordinate analysis (PCoA) plot.

4.4.4 Single molecules DDO methylation analyses in non-psychiatric subjects and patients with schizophrenia.

I then provided information about DDO epiallele classes distribution and epiallele distribution analyses. As for DAO, no significant differences were detected comparing SCZ and CTRL groups in all analyzed brain areas. However, I found that HIPP and CX displayed an epiallele classes distribution clearly different from CB area (Cramer test, $p < 0.001$), as expected by the lower DDO average methylation in CB. However, it was possible appreciate some peculiar differences in epiallele classes distribution from the comparison between HIPP and CX, especially for the 2-Meth class and 7-Meth class, both more abundant in DLPFC with respect to HIPP. Finally, I performed PCoA analysis pulling together the epiallele composition of all brain areas and SCZ and CTRL groups. Also in this case, epiallele distribution confirmed the cluster of CB away from HIPP and DLPFC, indicating a strong typing of CB cells compared to the other two brain areas. In conclusion, despite the inability in the detection of differences between CTRL and SCZ groups, also for DDO locus I identified specific methylation profiles distinguishing the different cell type composition in HIPP, DLPFC and CB.

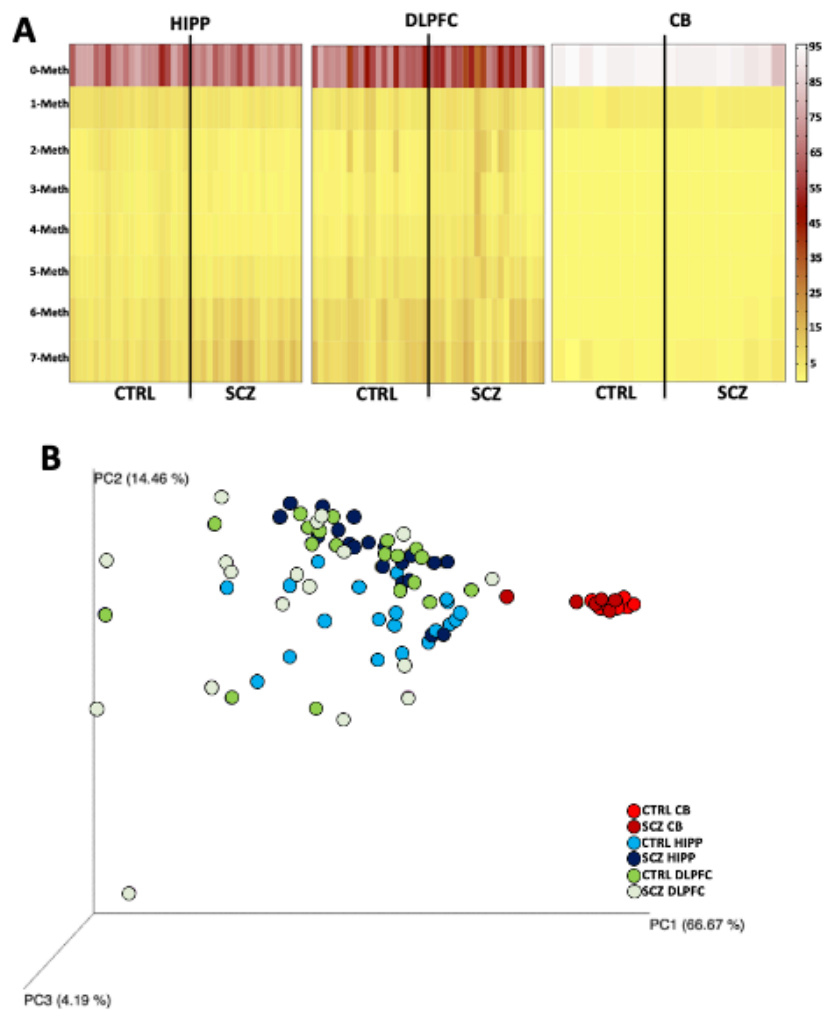


Figure 20. Epiallele classes and distribution analyses at human DDO gene. (A) Heatmaps show the abundance of all the different epiallele classes (from 0 to 10 methyl-cytosine per molecule) in each sample and in all analyzed brain regions (hippocampus = HIPP; dorsolateral prefrontal cortex = DLPFC; cerebellum = CB). The color gradient from yellow to white indicates the percentage of each epiallelic class. (B) Epialleles distribution analysis of the human DDO gene, taking in consideration all brain region and both groups, is shown in the principal coordinate analysis (PCoA) plot.

5. DISCUSSION

Several studies have successfully identified DNA methylation patterns and differentially methylated regions in health and disease (28-30, 48, 68, 69, 71, 87). The great majority of these studies, even when performed at high resolution, could measure the average methylation at each locus. However, the exact methylation profiling that establish during development and/or disease process remains still poor understood. In this study, I have applied different methods to study DNA methylation at high resolution at DAO and DDO gene loci both in physiological brain development and in post-mortem tissues from patients with schizophrenia. These two genes are responsible for the degradation of two D-amino acid that interact with NMDAR, D-Ser and D-Asp, respectively. Since D-Ser and D-Asp may be considered important brain neuromodulators, their levels in mammalian brain must be strictly controlled. Indeed, D-Asp levels are high during fetal life and drastically reduced in early post-natal period whereas D-Ser levels are more constant during life. Moreover, the levels of these two D-amino acids follow a specific brain regionality, being D-Ser more expressed in cerebellum and D-Asp more abundant in prefrontal cortex. Thus, considering the so fine spatio-temporal distribution of D-Ser and D-Asp, an alteration in the correct amount of these two D-amino acids has been linked to several neuropsychiatric conditions. In accordance, several SNPs identified at genes regulating D-amino acid metabolism have been linked to schizophrenia 20,51–53. A deficiency of D-Ser levels includes several symptoms such as epilepsy, spasticity, and neurocognitive disorders (Szilágyi B et al., 2018). Moreover, some symptoms of schizophrenia are due to a D-serine deregulation (Ma T et al., 2019) and the inhibition of DAO enzyme appears to have therapeutic potential (Kölker S, 2018). All these data suggest that an epigenetic mechanism may indirectly control the levels of D-Ser and D-Asp by regulating the enzymes involved in their degradation and synthesis. Based on the basic and translational interest of free D-amino acids in brain physiology and pathology, in my PhD thesis I have analyzed the spatio-temporal DNA methylation

dynamics at DAO and DDO genes via a single-molecule approach (epiallele distribution and epiallele classes analyses), in three different brain regions (HIPP, CX, and CB) at postnatal days P1, P15, P30, and P60. Moreover, I extended the same analysis to 3 different post-mortem tissues (HIPP, DLPFC and CB) from patients with schizophrenia. I found a physiological and selective demethylation event at DAO promoter during brain development specifically at two CpG sites and in cerebellum area. Moreover, this demethylation appeared to be much more effective in cerebellar astrocyte from P1 to P15. This dynamic demethylation phenomena resulted in progressive activation of DAO gene with a dramatic area-specific modulation of D-Ser. Some previous studies demonstrated that postnatal programmed demethylation at few CpG site plays a fundamental role in the regulation of glucocorticoid receptor gene expression and the absence of this event leads to persistent alteration of the HPA axis (Weaver ICG et al., 2004). Moreover, I demonstrated that the posthumous demethylation of few CpG sites is likely marked by 5-hmC, since I found that this intermediate compound of TET-mediated demethylation was enriched at the CpG sites undergoing demethylation at later developmental stages. Regarding D-Asp levels, in a recent study conducted on whole brain, the promoter of DDO gene is activated by DNA methylation decrease during development, with a concomitant decrease of D-Asp level (Florio et al., 2017). In my PhD studies I extended this analysis to the different brain regions and developmental stages. I found that this demethylation event occurs in HIPP and CB but not in CX, although the mRNA levels of this gene increase in all brain areas, including CX. Of particular interest, the strongest DDO gene activation appears in CB, where only two CpG sites (- 125 and - 175) remained demethylated over time, suggesting, also in this case, a critical role of few CpG sites in regulating genes. Altogether, the data obtained in mice brain areas at different developmental stages highlight the importance of post-natal changes of DNA methylation at few CpG sites in the proper control of D- Ser and D-Asp levels with potential clinical implications. For this reason, I decided to investigated DNA methylation

along with mRNA expression of DAO and DDO genes in post-mortem brain tissues in patients with schizophrenia. Despite the absence of core alterations between diagnosis groups, strong differences among the HIPP, DLPFC and CB brain areas were identified with clearly detectable methylation signatures. Also in this study, I performed epiallele analyses and especially at DAO gene, I identified cell to cell methylation differences. I found specific epiallelic profiles that, regardless of diagnosis, render the CB tissue clearly distinct from DLPFC and HIPP, likely suggesting a specific CpG combinatorial code that characterize cellular composition of different brain areas. Since the DNA methylation levels at DDO gene has been previously measured in patients with schizophrenia and non-psychiatric subjects (Keller et al., 2017), I extended the methylation analysis at DDO gene promoter in CB, and performed epiallele analyses on HIPP, DLPFC and CB. I observed a lower DNA methylation and expression at DDO locus in the CB compared to the HIPP and DLPFC. As expected by lower average methylation, epialleles classes analysis clearly and significantly distinguished from HIPP and DLPFC, as confirmed by the Cramer test ($p < 0.001$). Moreover, although sharing a similar average methylation, DLPFC and hippocampus displayed significant differences in epialleles classes distribution, especially in some intermediate classes. Considering the high power of this approach confirmed both in mouse and in human, epiallele analyses may represents a novel tool to detect fine differences in gene methylation distribution, otherwise not appreciated with classical targeted or genome-wide methods. Overall, the epigenetic diversity that I found at DAO and DDO gene may supports the possible existence of mechanisms oriented to maintain the epigenetic system in a dynamic stability, where the methylation state of each CpG in single cells is not stable but it is subject to periodic fluctuations.

6. CONCLUSION

My data strongly highlight the importance to investigate in detail the appropriate programmed DNA methylation events that indirectly control the levels of two important brain neurotransmitters, D-Ser and D-Asp. Particularly, the identification of an active demethylation process at DAO and DDO genes is fundamental for the maintenance of physiological D-Ser and D-Asp levels and thus, for correct brain development (Errico F et al., 2012; Katane M et al., 2011; Katane M et al., 2010; Wolosker H et al., 1999; Hashimoto A et al., 1993; Sakai K et al., 1998; Balu DT et al., 2012; Ivanov AD et al., 2018). Moreover, epiallele distribution analysis at these two genes allowed me to better characterize the methylation status of DAO and DDO promoter during the mouse brain development and to identify cell-to-cell methylation signatures able to recognize the different examined brain tissues. Very importantly, altered levels of D-Ser and D-Asp have been found in different neuropsychiatric conditions (Errico F et al., 2015; Hashimoto K et al., 2013; Sacchi S et al., 2013; Chang HJ et al., 2014; Coyle JT et al., 2017) and to contribute to these alterations, environmental factors may play a fundamental role. Thus, I hypothesized that non proper establishment in DNA methylation may have clinical impact in the etiopathogenesis and treatment of neurodevelopmental disorders. For this reason, I analyze DNA methylation at DAO and DDO genes in post-mortem tissues from patients with schizophrenia. The lack of significant methylation and expression changes in DAO and DDO genes between patients with schizophrenia and non-psychiatric controls could be due to the fact that schizophrenia has a multifactorial etiology. Moreover, given the small number of samples analyzed here, it is possible that an increased sample size is necessary to detect more subtle changes in gene expression. Another critical point to consider is the effect of potential confounding variables, such as post-mortem interval, age, and pH of the brain samples, even though statistical analyses showed that confounders did not affect the RNA expression and DNA methylation results (see Materials and Methods).

Interestingly, also in human, distinct area-specific patterns suggested the occurrence of an organized distribution of epialleles in different cell populations represented in each brain area. Since it is possible that the methylation state of the genes interrogated here varies between different cell types (i.e. excitatory and inhibitory neurons, astrocytes), there could be differences in SCZ if these diverse cell populations could be sorted prior to sequencing. Overall, we believe that at selected genes, epiallele-based analyses may be more informative than traditional methylation analyses and can be successfully utilized in a broad range of applications, including in depth determination of epigenetic origin of brain diseases. In addition, provided that these analyses are successfully transferable to peripheral cells, they may be applied for diagnostic and clinical purposes.

Acknowledgements

I wish to thank my tutor Prof. Lorenzo Chiariotti for his enormously precious advices and for having allowed my personal and professional growth. I thank Prof. Alessandro Usiello and his teams and Prof. Sergio Cocozza and his teams for their huge contribution to my PhD study. I would like to thank all members of lab, Dr. Lorena Coretti, Dr. Rosa Della Monica, Dr. Roberta Vinciguerra, Dr. Teodolinda Di Risi, Dr. Davide Costabile and Dr. Michela Buonaiuto for all the support given to me in these three years.

References

- Adams RLP. DNA methylation-The effect of minor bases on DNA-protein interactions. *Biochem J.* 265: 309-320. (1990)
- Affinito O, Scala G, Palumbo D, Florio E, Monticelli A, Miele G, Avvedimento VE, Usiello A, Chiariotti L, Coccozza S. Modeling DNA methylation by analyzing the individual configurations of single molecules. *Epigenetics.* 2016;11(12):881-888.
- Allfrey V, Faulkner RM, Mirsky AE. Acetylation and methylation of histones and their possible role in the regulation of RNA synthesis. *Proc Natl Acad Sci USA.* 1964;51: 786–794.
- Anastasiadou E, Jacob LS, Slack FJ. Non-coding RNA networks in cancer. *Nat Rev Cancer.* 2018;18(1):5-18. doi: 10.1038/nrc.2017.99.
- Balu DT, Coyle JT. Neuronal d-serine regulates dendritic architecture in the somatosensory cortex. *Neurosci Lett.* 2012;517(2):77–81.
- Balu DT, Coyle JT. The NMDA receptor ‘glycine modulatory site’ in schizophrenia: D-serine, glycine, and beyond. *Curr Opin Pharmacol.* 2015;109–115.
- Balu DT. The NMDA Receptor and Schizophrenia: From Pathophysiology to Treatment. *Adv Pharmacol.* 2016;76:351-382.
- Beasley CL, Honer WG, Ramos-Miguel A, Vila-Rodriguez F, Barr AM. Prefrontal fatty acid composition in schizophrenia and bipolar disorder: Association with reelin expression. *Schizophr Res.* 2020;215:493-498.
- Becker PB. The establishment of active promoters in chromatin. *Bioessays.* 1994; 16: 541–547.
- Bendikov I, Nadri C, Amar S, Panizzutti R, De Miranda J, Wolosker H, Agam G. A CSF and postmortem brain study of D-serine metabolic parameters in schizophrenia. *Schizophr Res.* 2007;90(1-3):41-51.

Bird A. DNA methylation patterns and epigenetic memory. *Genes Dev.* 2002;16(1):6-21.

Boland MJ, Nazor KL, Loring JF. Epigenetic regulation of pluripotency and differentiation. *Circ Res.* 2014;115(2):311-24.

Booth MJ, Ost TW, Beraldi D, Bell NM, Branco MR, Reik W, Balasubramanian S. Oxidative bisulfite sequencing of 5-methylcytosine and 5-hydroxymethylcytosine. *Nat Protoc.* 2013;8(10):1841–51.

Borgel J, Guibert S, Li Y, Chiba H, Schübeler D, Sasaki H, Forné T, Weber M. Targets and dynamics of promoter DNA methylation during early mouse development. *Nature Publishing Group.* 2010;42: 1093–1100.

Breiling A, Lyko F. Epigenetic regulatory functions of DNA modifications: 5-methylcytosine and beyond. *Epigenetics Chromatin.* 2015;8:24.

Calcia MA, Madeira C, Alheira FV, Silva TC, Tannos FM, Vargas-Lopes C, Goldenstein N, Brasil MA, Ferreira ST, Panizzutti R. Plasma levels of D-serine in Brazilian individuals with schizophrenia. *Schizophr Res.* 2012;142(1-3):83-7

Camacho C, Coulouris G, Avagyan V, Ma N, Papadopoulos J, Bealer K, Madden TL. BLAST+: architecture and applications. *BMC Bioinformatics* 2009;10: 421

Chang HJ, Lane HY, Tsai GE. NMDA pathology and treatment of schizophrenia. *Curr Pharm Des.* 2014;20(32):5118–26.

Chen T, Ueda Y, Dodge JE, Wang Z, Li E. Establishment and maintenance of genomic methylation patterns in mouse embryonic stem cells by Dnmt3a and Dnmt3b. *Mol. Cell. Biol.* 2003;23:5594–5605.

Clouaire T, Stancheva I. Methyl-CpG binding proteins: specialized transcriptional repressors or structural components of chromatin? *Cell Mol Life Sci.* 2008;65(10):1509-22.

Costa E, Chen Y, Davis J, Dong E, Noh JS, Tremolizzo L, Veldic M, Grayson DR, Guidotti A. REELIN and schizophrenia: a disease at the interface of the genome and the epigenome. *Mol Interv.* 2002;2(1):47-57.

Cotton AM, Lam L, Affleck JG, Wilson IM, Peñaherrera MS, McFadden DE, KoborMS, Lam WL, Robinson WP, Brown CJ. Chromosome-wide DNA methylation analysis predicts human tissue- specific X inactivation. *Hum Genet.* 2011;130(2):187-201.

Coyle JT, Balu DT. The role of serine racemase in the pathophysiology of brain disorders. *Adv Pharmacol.* 2017;82:35–56.

Coyle JT. NMDA receptor and schizophrenia: a brief history. *Schizophr Bull.* 2012;38, 920–926.

Cuomo M, Keller S, Punzo D, Nuzzo T, Affinito O, Coretti L, Carella M, de Rosa V, Florio E, Boscia F, Avvedimento VE, Coccozza S, Errico F, Usiello A, Chiariotti L. Selective demethylation of two CpG sites causes postnatal activation of the Dao gene and consequent removal of D-serine within the mouse cerebellum. *Clin Epigenetics.* 2019;11(1):149.

Dawlaty MM, Breiling A, Le T, Barrasa MI, Raddatz G, Gao Q, Powell BE, Cheng AW, Faull KF, Lyko F, Jaenisch R. Loss of Tet enzymes compromises proper differentiation of embryonic stem cells. *Dev Cell.* 2014;29(1):102-11.
Deaton AM, Bird A. CpG islands and the regulation of transcription. *Genes Dev.* 2011;25(10):1010-22.

Derrien T, Johnson R, Bussotti G, Tanzer A, Djebali S, Tilgner H, Guernec G, Martin D, Merkel A, Knowles DG, Lagarde J, Veeravalli L, Ruan X, Ruan Y, Lassmann T, Carninci P, Brown JB, Lipovich L, Gonzalez JM, Thomas M, Davis CA, Shiekhattar R, Gingeras TR, Hubbard TJ, Notredame C, Harrow J, Guigó R. The GENCODE v7 catalog of human long noncoding RNAs: analysis of their gene structure, evolution, and expression. *Genome Res.* 2012;22(9):1775-89.

Errico F, Cuomo M, Canu N, Caputo V, Usiello A. New insights on the influence of free d-aspartate metabolism in the mammalian brain during prenatal and postnatal life. *Biochim Biophys Acta Proteins Proteom.* 2020;1868(10):140471.

Errico F, Mothet JP, Usiello A. D-aspartate: an endogenous NMDA receptor agonist enriched in the developing brain with potential involvement in schizophrenia. *J Pharm Biomed Anal.* 2015;116:7–17.

Errico F, Napolitano F, Nisticò R, Usiello A. New insights on the role of free D-aspartate in the mammalian brain. *Amino Acids*. 2012;43(5):1861–71.

Errico F, Napolitano F, Squillace M, Vitucci D, Blasi G, de Bartolomeis A, Bertolino A, D'Aniello A, Usiello A. Decreased levels of D-aspartate and NMDA in the prefrontal cortex and striatum of patients with schizophrenia. *J Psychiatr Res*. 2013;47(10):1432-7.

Errico F, Pirro MT, Affuso A, Spinelli P, De Felice M, D'Aniello A, Di Lauro R. A physiological mechanism to regulate D-aspartic acid and NMDA levels in mammals revealed by D-aspartate oxidase deficient mice. *Gene*. 2016;374:50 – 57.

Fan G, Hutnick L. Methyl-CpG binding proteins in the nervous system. *Cell Res*. 2005;15(4):255-61.

Farhy-Tselnicker I, Allen NJ. Astrocytes, neurons, synapses: a tripartite view on cortical circuit development. *Neural Dev*. 2018;13(1):7.

Farrell C, Doolin K, O' Leary N, Jairaj C, Roddy D, Tozzi L, Morris D, Harkin A, Frodl T, Nemoda Z, Szyf M, Booij L, O'Keane V. DNA methylation differences at the glucocorticoid receptor gene in depression are related to functional alterations in hypothalamic-pituitary-adrenal axis activity and to early life emotional abuse. *Psychiatry Res*. 2018 Jul;265:341-348.

Fatica A, Bozzoni I. Long non-coding RNAs: new players in cell differentiation and development. *Nat Rev Genet*. 2014;15(1):7-21.

Feng J, Zhou Y, Campbell SL, Le T, Li E, Sweatt JD, Silva AJ, Fan G. Dnmt1 and Dnmt3a maintain DNA methylation and regulate synaptic function in adult forebrain neurons. *Nat Neurosci*. 2010;13(4):423-30.

Feng Q, Zhang H, Yao D, Chen WD, Wang YD. Emerging Role of Non-Coding RNAs in Esophageal Squamous Cell Carcinoma. *Int J Mol Sci*. 2019;21(1):258.

Florio E, Keller S, Coretti L, Affinito O, Scala G, Errico F, Fico A, Boscia F, Sisalli MJ, Reccia MG, Miele G, Monticelli A, Scorziello A, Lembo F, Colucci-D'Amato L, Minchiotti G, Avvedimento VE, Usiello A, Coccozza S, Chiariotti L. Tracking the evolution of epialleles during neural differentiation and brain

development: D-Aspartate oxidase as a model gene. *Epigenetics*. 2017;12(1):41-54.

Fouse SD, Nagarajan RO, Costello JF. Genome-scale DNA methylation analysis. *Epigenomics*. 2010;2(1):105-117.

Gökbuget D, Blesloch R. Epigenetic control of transcriptional regulation in pluripotency and early differentiation. *Development*. 2019;146(19):dev164772.

Goldberg AD, Allis CD, Bernstein E. Epigenetics: a landscape takes shape. *Cell*. 2007;128(4):635-8.

Guibert S, Weber M. Epigenetics: erase for a new start. *Nature*. 2012;492: 363–364.

Guo W, Zhang MQ, Wu H. Mammalian non-CG methylations are conserved and cell-type specific and may have been involved in the evolution of transposon elements. *Sci Rep*. 2016;6:32207.

Habl G, Schmitt A, Zink M, von Wilmsdorff M, Yeganeh-Doost P, Jatzko A, Schneider-Axmann T, Bauer M, Falkai P. Decreased reelin expression in the left prefrontal cortex (BA9) in chronic schizophrenia patients. *Neuropsychobiology*. 2012;66(1):57-62.

Habl G, Zink M, Petroianu G, Bauer M, Schneider-Axmann T, von Wilmsdorff M, Falkai P, Henn FA, Schmitt A. Increased D-amino acid oxidase expression in the bilateral hippocampal CA4 of schizophrenic patients: a post-mortem study. *J Neural Transm (Vienna)*. 2009;116(12):1657-65.

Hajkova P, Erhardt S, Lane N, Haaf T, El-Maarri O, Reik W, Walter J, Surani MA. Epigenetic reprogramming in mouse primordial germ cells. *Mech Dev*. 2002;117: 15–23.

Hashimoto A, Kumashiro S, Nishikawa T, Oka T, Takahashi K, Mito T, Takashima S, Doi N, Mizutani Y, Yamazaki T, et al. Embryonic development and postnatal changes in free D-aspartate and D-serine in the human prefrontal cortex. *J Neurochem*. 1993;61(1):348-51.

Hashimoto A, Oka T, Nishikawa T. Anatomical distribution and postnatal changes in endogenous free D-aspartate and D-serine in rat brain and periphery. *Eur J Neurosci.* 1995;7(8):1657-63.

Hashimoto A, Oka T. Free D-aspartate and D-serine in the mammalian brain and periphery. *Prog Neurobiol.* 1997;52(4):325-53.

Hashimoto K, Engberg G, Shimizu E, Nordin C, Lindström LH, Iyo M. Reduced D-serine to total serine ratio in the cerebrospinal fluid of drug naive schizophrenic patients. *Prog Neuropsychopharmacol Biol Psychiatry.* 2005;29(5):767-9.

Hashimoto K, Fukushima T, Shimizu E, Komatsu N, Watanabe H, Shinoda N, Nakazato M, Kumakiri C, Okada S, Hasegawa H, Imai K, Iyo M. Decreased serum levels of D-serine in patients with schizophrenia: evidence in support of the N-methyl-D-aspartate receptor hypofunction hypothesis of schizophrenia. *Arch Gen Psychiatry.* 2003;60(6):572-6.

Hashimoto K, Malchow B, Falkai P, Schmitt A. Glutamate modulators as potential therapeutic drugs in schizophrenia and affective disorders. *Eur Arch Psychiatry Clin Neurosci.* 2013;263(5):367-77.

Henikoff S, Matzke MA. Exploring and explaining epigenetic effects. *Trends Genet.* 1997;13(8):293-5.

Hirota Y, Nakajima K. Control of Neuronal Migration and Aggregation by Reelin Signaling in the Developing Cerebral Cortex. *Front Cell Dev Biol.* 2017;5:40.

Holliday R. Epigenetics: a historical overview. *Epigenetics.* 2006;1(2):76-80.

Hu TM, Hsu SH, Tsai SM, Cheng MC. DNA methylation analysis of the EGR3 gene in patients of schizophrenia. *Psychiatry Res.* 2017;251:115-117.

Hyun K, Jeon J, Park K, Kim J. Writing, erasing and reading histone lysine methylations. *Exp Mol Med.* 2017;49(4):e324.

Ivanov AD, Mothet JP. The plastic d-serine signaling pathway: sliding from neurons to glia and vice-versa. *Neurosci Lett.* 2018;689:21-5.

Jaenisch R, Bird A. Epigenetic regulation of gene expression: how the genome integrates intrinsic and environmental signals. *Nat Genet.* 2003;33 Suppl:245-54.

Jaffe AE, Gao Y, Deep-Soboslay A, Tao R, Hyde TM, Weinberger DR, Kleinman JE. Mapping DNA methylation across development, genotype and schizophrenia in the human frontal cortex. *Nat Neurosci.* 2016;19(1):40-7.

Jagannath V, Gerstenberg M, Correll CU, Walitza S, Grünblatt E. A systematic meta-analysis of the association of Neuregulin 1 (NRG1), D-amino acid oxidase (DAO), and DAO activator (DAOA)/G72 polymorphisms with schizophrenia. *J Neural Transm (Vienna).* 2018;125(1):89-102.

Jagannath V, Marinova Z, Monoranu CM, Walitza S, Grünblatt E. Expression of D-Amino Acid Oxidase (DAO/DAAO) and D-Amino Acid Oxidase Activator (DAOA/G72) during Development and Aging in the Human Post-mortem Brain. *Front Neuroanat.* 2017;11:31.

Jenuwein T, Allis CD. Translating the histone code. *Science.* 2001;293(5532):1074-80.

Jin J, Lian T, Gu C, Yu K, Gao YQ, Su XD. The effects of cytosine methylation on general transcription factors. *Sci Rep.* 2016;6:29119.

Jones PA. Functions of DNA methylation: Islands, start sites, gene bodies and beyond. *Nat. Rev. Genet.* 2012;13:484–492.

Kaikkonen MU, Lam MT, Glass CK. Non-coding RNAs as regulators of gene expression and epigenetics. *Cardiovasc Res.* 2011;90(3):430- 40.

Katane M, Homma H. D-aspartate oxidase: the sole catabolic enzyme acting on free D-aspartate in mammals. *Chem Biodivers.* 2010;7(6):1435–49.

Katane M, Homma H. D-aspartate: an important bioactive substance in mammals: a review from an analytical and biological point of view. *J Chromatogr B Anal Technol Biomed Life Sci.* 2011;879(29):3108–21.

Keller S, Punzo D, Cuomo M, Affinito O, Coretti L, Sacchi S, Florio E, Lembo F, Carella M, Copetti M, Coccozza S, Balu DT, Errico F, Usiello A, Chiariotti L.

DNA methylation landscape of the genes regulating D-serine and D-aspartate metabolism in post-mortem brain from controls and subjects with schizophrenia. *Sci Rep.* 2018;8(1):10163.

Keller S, Sarchiapone M, Zarrilli F, Videtic A, Ferraro A, Carli V, Sacchetti S, Lembo F, Angiolillo A, Jovanovic N, Pisanti F, Tomaiuolo R, Monticelli A, Balazic J, Roy A, Marusic A, Coccozza S, Fusco A, Bruni CB, Castaldo G, Chiariotti L. Increased BDNF promoter methylation in the Wernicke area of suicide subjects. *Arch Gen Psychiatry.* 2010;67(3):258-67.

Kiriyama Y, Nochi H. d-Amino acids in the nervous and endocrine systems. *Scientifica (Cairo)*, 2016, Article 6494621

Kölker S. Metabolism of amino acid neurotransmitters: the synaptic disorder underlying inherited metabolic diseases. *J Inher Metab Dis.* 2018;41(6): 1055.

Konki M, Malonzo M, Karlsson IK, Lindgren N, Ghimire B, Smolander J, Scheinin NM, Ollikainen M, Laiho A, Elo LL, Lönnberg T, Røyttä M, Pedersen NL, Kaprio J, Lähdesmäki H, Rinne JO, Lund RJ. Peripheral blood DNA methylation differences in twin pairs discordant for Alzheimer's disease. *Clin Epigenetics.* 2019;11(1):130.

Kouzarides T. Chromatin modifications and their function. *Cell.* 2007;128: 693–705

Kribelbauer JF, Lu XJ, Rohs R, Mann RS, Bussemaker HJ. Toward a Mechanistic Understanding of DNA Methylation Readout by Transcription Factors. *J Mol Biol.* 2019:S0022-2836(19)30617-5.

Labonté B, Suderman M, Maussion G, Navaro L, Yerko V, Mahar I, Bureau A, Mechawar N, Szyf M, Meaney MJ, Turecki G. Genome-wide epigenetic regulation by early-life trauma. *Arch. Gen. Psychiatry.* 2012;69, 722-731.

Landan G, Cohen NM, Mukamel Z, Bar A, Molchadsky A, Brosh R, Horn-Saban S, Zalcenstein DA, Goldfinger N, Zundeleovich A, Gal-Yam EN, Rotter V, Tanay A. Epigenetic polymorphism and the stochastic formation of differentially methylated regions in normal and cancerous tissues. *Nat Genet.* 2012;44(11):1207-14.

Leonhardt H, Page AW, Weier H-U, Bestor TH. A targeting sequence directs DNA methyltransferase to sites of DNA replication in mammalian nuclei. *Cell*. 1992;71:865–873.

Li S, Garrett-Bakelman F, Perl AE, Luger SM, Zhang C, To BL, Lewis ID, Brown AL, D'Andrea RJ, Ross ME, Levine R, Carroll M, Melnick A, Mason CE. Dynamic evolution of clonal epialleles revealed by methclone. *Genome Biol*. 2014;15(9):472.

Li S, Zong L, Hou Y, Zhang W, Zhou L, Yang Q, Wang L, Jiang W, Li Q, Huang X, Ning Y, Wen Z, Zhao C. Altered DNA methylation of the AluY subfamily in schizophrenia and bipolar disorder. *Epigenomics*. 2019;11(6):581-586.

Liao J, Karnik R, Gu H, Ziller MJ, Clement K, Tsankov AM, Akopian V, Gifford CA, Donaghey J, Galonska C, Pop R, Reyon D, Tsai SQ, Mallard W, Joung JK, Rinn JL, Gnirke A, Meissner A. Targeted disruption of DNMT1, DNMT3A and DNMT3B in human embryonic stem cells. *Nat Genet*. 2015;47(5):469-78.

Lister R, Mukamel EA, Nery JR, Urich M, Puddifoot CA, Johnson ND, Lucero J, Huang Y, Dwork AJ, Schultz MD, Yu M, Tonti-Filippini J, Heyn H, Hu S, Wu JC, Rao A, Esteller M, He C, Haghghi FG, Sejnowski TJ, Behrens MM, Ecker JR. Global epigenomic reconfiguration during mammalian brain development. *Science*. 2013;341(6146):1237905.

Liu Y, Oakeley EJ, Sun L, Jost J-P. Multiple domains are involved in the targeting of the mouse DNA methyltransferase to the DNA replication foci. *Nucleic Acids Res*. 1998;26:1038–1045.

Liu YL, Wang SC, Hwu HG, Fann CS, Yang UC, Yang WC, Hsu PC, Chang CC, Wen CC, Tsai-Wu JJ, Hwang TJ, Hsieh MH, Liu CC, Chien YL, Fang CP, Faraone SV, Tsuang MT, Chen WJ, Liu CM. Haplotypes of the D-Amino Acid Oxidase Gene Are Significantly Associated with Schizophrenia and Its Neurocognitive Deficits. *PLoS One*. 2016;11(3):e0150435.

Ma T, Wu Y, Chen B, Zhang W, Jin L, Shen C, et al. D-serine contributes to seizure development via ERK signaling. *Front Neurosci*. 2019;13:254.

Marzan S, Aziz MA, Islam MS. Association Between REELIN Gene Polymorphisms (rs7341475 and rs262355) and Risk of Schizophrenia: an Updated Meta-analysis. *J Mol Neurosci*. 2021;71(4):675-690.

Mattick JS, Makunin IV. Non-coding RNA. *Hum Mol Genet.* 2006;15 Spec No 1:R17-29.

Meier K, Recillas-Targa F. New insights on the role of DNA methylation from a global view. *Front Biosci (Landmark Ed).* 2017;22:644-668.

Mens MMJ, Ghanbari M. Cell Cycle Regulation of Stem Cells by MicroRNAs. *Stem Cell Rev Rep.* 2018;14(3):309-322.

Miller,G. Epigenetics. The seductive allure of behavioral epigenetics. *Science.* 2010;329, 24-27.

Miyoshi Y, Konno R, Sasabe J, Ueno K, Tojo Y, Mita M, Aiso S, Hamase K. Alteration of intrinsic amounts of D-serine in the mice lacking serine racemase and D-amino acid oxidase. *Amino Acids.* 2012;43(5):1919-31.

Mohammad F, Pandey GK, Mondal T, Enroth S, Redrup L, Gyllensten U, Kanduri C. Long noncoding RNA-mediated maintenance of DNA methylation and transcriptional gene silencing. *Development.* 2012;139(15):2792-803.

Mohn F, Weber M, Rebhan M, Roloff TC, Richter J, Stadler MB, Bibel M, Schübeler D. Lineage-specific polycomb targets and de novo DNA methylation define restriction and potential of neuronal progenitors. *Mol Cell.* 2008;30(6):755-66.

Moretti P, Levenson JM, Battaglia F, Atkinson R, Teague R, Antalffy B, Armstrong D, Arancio O, Sweatt JD, Zoghbi HY. Learning and memory and synaptic plasticity are impaired in a mouse model of Rett syndrome. *J Neurosci.* 2006;26(1):319-27

Morita Y, Ujike H, Tanaka Y, Otani K, Kishimoto M, Morio A, Kotaka T, Okahisa Y, Matsushita M, Morikawa A, Hamase K, Zaitzu K, Kuroda S. A genetic variant of the serine racemase gene is associated with schizophrenia. *Biol Psychiatry.* 2007;61(10):1200-3.

Nabil Fikri RM, Norlelawati AT, Nour El-Huda AR, Hanisah MN, Kartini A, Norsidah K, Nor Zamzila A. Reelin (RELN) DNA methylation in the peripheral blood of schizophrenia. *J Psychiatr Res.* 2017;88:28-37.

Nestler EJ, Peña CJ, Kundakovic M, Mitchell A, Akbarian S. Epigenetic Basis of Mental Illness. *Neuroscientist*. 2015;pii: 1073858415608147.

Nuzzo T, Sacchi S, Errico F, Keller S, Palumbo O, Florio E, Punzo D, Napolitano F, Copetti M, Carella M, Chiariotti L, Bertolino A, Pollegioni L, Usiello A. Decreased free d-aspartate levels are linked to enhanced d-aspartate oxidase activity in the dorsolateral prefrontal cortex of schizophrenia patients. *NPJ Schizophr*. 2017;3:16.

Okano M, Bell DW, Haber DA, Li E. DNA methyltransferases Dnmt3a and Dnmt3b are essential for de novo methylation and mammalian development. *Cell*. 1999;99(3):247-57.

Ono K, Shishido Y, Park HK, Kawazoe T, Iwana S, Chung SP, Abou El-Magd RM, Yorita K, Okano M, Watanabe T, Sano N, Bando Y, Arima K, Sakai T, Fukui K. Potential pathophysiological role of D-amino acid oxidase in schizophrenia: immunohistochemical and in situ hybridization study of the expression in human and rat brain. *J Neural Transm (Vienna)*. 2009;116(10):1335-47.

Patil V, Ward RL, Hesson LB. The evidence for functional non-CpG methylation in mammalian cells. *Epigenetics*. 2014;9(6):823-8.

Perroud N, Salzmann A, Prada P, Nicastro R, Hoeppli ME, Furrer S, Ardu S, Krejci I, Karege F, Malafosse A. Response to psychotherapy in borderline personality disorder and methylation status of the BDNF gene. *Transl Psychiatry*. 2013;3, e207.

Pfeifer GP, Kadam S, Jin SG. 5-hydroxymethylcytosine and its potential roles in development and cancer. *Epigenetics Chromatin*. 2013;6:10. doi: 10.1186/1756-8935-6-10.

Pollegioni L, Sacchi S. Metabolism of the neuromodulator D-serine. *Cell Mol Life Sci*. 2010;67(14):2387–404.

Popp C, Dean W, Feng S, Cokus SJ, Andrews S, Pellegrini M, Jacobsen SE, Reik W. Genome-wide erasure of DNA methylation in mouse primordial germ cells is affected by AID deficiency. *Nature*. 2010;463: 1101–1105.

Punzo D, Errico F, Cristino L, Sacchi S, Keller S, Belardo C, Luongo L, Nuzzo T, Imperatore R, Florio E, De Novellis V, Affinito O, Migliarini S, Maddaloni G, Sisalli MJ, Pasqualetti M, Pollegioni L, Maione S, Chiariotti L, Usiello A. Age-Related Changes in D-Aspartate Oxidase Promoter Methylation Control Extracellular D-Aspartate Levels and Prevent Precocious Cell Death during Brain Aging. *J Neurosci.* 2016;36(10):3064-78.

Qu W, Tsukahara T, Nakamura R, Yurino H, Hashimoto S, Tsuji S, Takeda H, Morishita S. Assessing Cell-to-Cell DNA Methylation Variability on Individual Long Reads. *Sci Rep.* 2016;6:21317.

Quina AS, Buschbeck M, Di Croce L. Chromatin structure and epigenetics. *Biochem Pharmacol.* 2006;72(11):1563-9

Raiber EA, Hardisty R, van Delft P, Balasubramanian S. Mapping and elucidating the function of modified bases in DNA. *Nat. Rev. Chem.* 2017;1
Rasmussen KD, Helin K. Role of TET enzymes in DNA methylation, development, and cancer. *Genes Dev.* 2016;30:733–750.

Razin A, Riggs AD. DNA methylation and gene function. *Science.* 1980;210:604–610.

Reimer M Jr, Pulakanti K, Shi L, Abel A, Liang M, Malarkannan S, Rao S. Deletion of Tet proteins results in quantitative disparities during ESC differentiation partially attributable to alterations in gene expression. *BMC Dev Biol.* 2019;19(1):16.

Sacchi S, Rosini E, Pollegioni L, Molla G. D-amino acid oxidase inhibitors as a novel class of drugs for schizophrenia therapy. *Curr Pharm Des.* 2013;19(14):2499–511

Sakai K, Homma H, Lee JA, Fukushima T, Santa T, Tashiro K, Iwatsubo T, Imai K. Emergence of D-aspartic acid in the differentiating neurons of the rat central nervous system. *Brain Res.* 1998;808(1):65-71.

Santiago M, Antunes C, Guedes M, Sousa N, Marques CJ. TET enzymes and DNA hydroxymethylation in neural development and function - how critical are they? *Genomics.* 2014;104(5):334-40.

Scala G, Affinito O, Palumbo D, Florio E, Monticelli A, Miele G, Chiariotti L, Cocozza S. ampliMethProfiler: a pipeline for the analysis of CpG methylation profiles of targeted deep bisulfite sequenced amplicons. *BMC Bioinformatics*. 2016;17(1):484.

Schell MJ, Molliver ME, Snyder SH. D-serine, an endogenous synaptic modulator: localization to astrocytes and glutamate-stimulated release. *Proc Natl Acad Sci*. 1995;92(9):3948–52.

Schmieder R, Edwards R. Quality control and preprocessing of metagenomic datasets. *Bioinformatics* 2011;27: 863-4.

Smith ZD, Meissner A. DNA methylation: roles in mammalian development. *Nat Rev Genet*. 2013;14(3):204-20.

Sozuguzel MD, Sazci A, Yildiz M. Female gender specific association of the Reelin (RELN) gene rs7341475 variant with schizophrenia. *Mol Biol Rep*. 2019;46(3):3411-3416.

Stoccoro A, Coppedè F. Role of epigenetics in Alzheimer's disease pathogenesis. *Neurodegener Dis Manag*. 2018;8(3):181-193.

Strahl BD, Allis CD. The language of covalent histone modifications. *Nature*. 2000; 403(6765):41-5.

Szilágyi B, Ferenczy GG, Keserű GM. Drug discovery strategies and the preclinical development of D-amino-acid oxidase inhibitors as antipsychotic therapies. *Expert Opin Drug Discov*. 2018;13(10):973–82.

Theunissen TW, Jaenisch R. Mechanisms of gene regulation in human embryos and pluripotent stem cells. *Development*. 2017;144(24):4496-4509.

Tsankova N, Renthal W, Kumar A, Nestler EJ. Epigenetic regulation in psychiatric disorders. *Nat Rev Neurosci*. 2007;8(5):355-67.

Uysal F, Ozturk S, Akkoyunlu G. DNMT1, DNMT3A and DNMT3B proteins are differently expressed in mouse oocytes and early embryos. *J Mol Histol*. 2017;48(5-6):417-426.

Veland N, Lu Y, Hardikar S, Gaddis S, Zeng Y, Liu B, Estecio MR, Takata Y, Lin K, Tomida MW, Shen J, Saha D, Gowher H, Zhao H, Chen T. DNMT3L facilitates DNA methylation partly by maintaining DNMT3A stability in mouse embryonic stem cells. *Nucleic Acids Res.* 2019;47(1):152-167.

Verrall L, Burnet PW, Betts JF, Harrison PJ. The neurobiology of D-amino acid oxidase and its involvement in schizophrenia. *Mol Psychiatry.* 2010;15(2):122-37.

Verrall L, Walker M, Rawlings N, Benzel I, Kew JN, Harrison PJ, Burnet PW. d-Amino acid oxidase and serine racemase in human brain: normal distribution and altered expression in schizophrenia. *Eur J Neurosci.* 2007;26(6):1657-69.
Wang KC, Chang HY. Molecular mechanisms of long noncoding RNAs. *Mol Cell.* 2011;43(6):904-14.

Weaver IC, Cervoni N, Champagne FA, D'Alessio AC, Sharma S, Seckl JR, Dymov S, Szyf M, Meaney MJ. Epigenetic programming by maternal behavior. *Nat Neurosci.* 2004;7(8):847-54.

Weaver JR, Susiarjo M, Bartolomei MS. Imprinting and epigenetic changes in the early embryo. *Mamm Genome.* 2009;20(9- 10):532-43.

Wei X, Zhang L, Zeng Y. DNA methylation in Alzheimer's disease: In brain and peripheral blood. *Mech Ageing Dev.* 2020;191:111319

Williams K, Christensen J, Helin K. DNA methylation: TET proteins-guardians of CpG islands? *EMBO Rep.* 2011;13:28–35.

Wolosker H, Blackshaw S, Snyder SH. Serine racemase: a glial enzyme synthesizing D-serine to regulate glutamate-N-methyl-D-aspartate neurotransmission. *Proc Natl Acad Sci U S A.* 1999;96(23):13409–14.

Wood LS, Pickering EH, Dechairo BM. Significant support for DAO as a schizophrenia susceptibility locus: examination of five genes putatively associated with schizophrenia. *Biol Psychiatry.* 2007;61(10):1195-9.

Wu X, Zhang Y. TET-mediated active DNA demethylation: Mechanism, function and beyond. *Nat. Rev. Genet.* 2017;18:517–534.

- Xie S, Li E. Cloning and characterization of a family of novel mammalian DNA (cytosine-5) methyltransferases. *Nat Genet.* 1998;19(3):219-20.
- Xin Y, O'Donnell AH, Ge Y, Chanrion B, Milekic M, Rosoklija G, Stankov A, Arango V, Dwork AJ, Gingrich JA, Haghghi FG. Role of CpG context and content in evolutionary signatures of brain DNA methylation. *Epigenetics.* 2011;6(11):1308-18.
- Yamada K, Ohnishi T, Hashimoto K, Ohba H, Iwayama-Shigeno Y, Toyoshima M, Okuno A, Takao H, Toyota T, Minabe Y, Nakamura K, Shimizu E, Itokawa M, Mori N, Iyo M, Yoshikawa T. Identification of multiple serine racemase (SRR) mRNA isoforms and genetic analyses of SRR and DAO in schizophrenia and D-serine levels. *Biol Psychiatry.* 2005;57(12):1493-503.
- Yamada M, Yamada M, Higuchi T. Antidepressant-elicited changes in gene expression: remodeling of neuronal circuits as a new hypothesis for drug efficacy. *Prog Neuropsychopharmacol Biol Psychiatry.* 2005;29(6), 999–1009.
- Yan P, Luo S, Lu JY, Shen X. Cis- and trans-acting lncRNAs in pluripotency and reprogramming. *Curr Opin Genet Dev.* 2017;46:170-178.
- Yang HC, Liu CM, Liu YL, Chen CW, Chang CC, Fann CS, Chiou JJ, Yang UC, Chen CH, Faraone SV, Tsuang MT, Hwu HG. The DAO gene is associated with schizophrenia and interacts with other genes in the Taiwan Han Chinese population. *PLoS One.* 2013;8(3):e60099.
- Yang XJ, Seto E. HATs and HDACs: from structure, function and regulation to novel strategies for therapy and prevention. *Oncogene* 2007;5310–5318.
- Yen RW, Vertino PM, Nelkin BD, Yu JJ, el-Deiry W, Cumaraswamy A, Lennon GG, Trask BJ, Celano P, Baylin SB. Isolation and characterization of the cDNA encoding human DNA methyltransferase. *Nucleic Acids Res.* 1992;20(9):2287-91.
- Zeng Y, Chen T. DNA Methylation Reprogramming during Mammalian Development. *Genes (Basel).* 2019;10(4):257.
- Zhang J, Kobert K, Flouri T, Stamatakis A. PEAR: a fast and accurate Illumina Paired-End reAd mergeR. *Bioinformatics* 2013;30: 614-20

Zhu H, Wang G, Qian J. Transcription factors as readers and effectors of DNA methylation. *Nat Rev Genet.* 2016;17(9):551-65.

List of publications

I. Boccella N, Paolillo R, Coretti L, D'Apice S, Lama A, Giugliano G, Schiattarella GG, **Cuomo M**, d'Aquino I, Cavaliere G, Paciello O, Mollica MP, Mattace Raso G, Esposito G, Lembo F, Perrino C. Transverse aortic constriction induces gut barrier alterations, microbiota remodeling and systemic inflammation. *Sci Rep.* 2021;11(1):7404.

II. Di Risi T, Vinciguerra R, **Cuomo M**, Della Monica R, Riccio E, Coccozza S, Imbriaco M, Duro G, Pisani A, Chiariotti L. DNA methylation impact on Fabry disease. *Clin Epigenetics.* 2021 Feb 2;13(1):24

III. **Cuomo M**, Borrelli L, Della Monica R, Coretti L, De Riso G, D'Angelo Lancellotti di Durazzo L, Fioretti A, Lembo F, Dinan TG, Cryan JF, Coccozza S, Chiariotti L. DNA Methylation Profiles of Tph1A and BDNF in Gut and Brain of L. Rhamnosus-Treated Zebrafish. *Biomolecules.* 2021 Jan 22;11(2):142.

IV. Citraro R, Lembo F, De Caro C, Tallarico M, Coretti L, Iannone LF, Leo A, Palumbo D, **Cuomo M**, Buommino E, Nesci V, Marascio N, Iannone M, Quirino A, Russo R, Calignano A, Constanti A, Russo E, De Sarro G. First evidence of altered microbiota and intestinal damage and their link to absence epilepsy in a genetic animal model, the WAG/Rij rat. *Epilepsia.* 2021 Feb;62(2):529-541.

V. De Riso G, Fiorillo DFG, Fierro A, **Cuomo M**, Chiariotti L, Miele G, Coccozza S. Modeling DNA Methylation Profiles through a Dynamic Equilibrium between Methylation and Demethylation. *Biomolecules.* 2020 Sep 3;10(9):1271.

VI. Pezone A, Tramontano A, Scala G, **Cuomo M**, Riccio P, De Nicola S, Porcellini A, Chiariotti L, Avvedimento EV. Tracing and tracking epiallele families in complex DNA populations. *NAR Genom Bioinform.* 2020 Nov 16;2(4):lqaa096.

VII. Errico F, **Cuomo M**, Canu N, Caputo V, Usiello A. New insights on the influence of free d-aspartate metabolism in the mammalian brain during prenatal and postnatal life. *Biochim Biophys Acta Proteins Proteom.* 2020 Oct;1868(10):140471.

VIII. De Riso G, **Cuomo M**, Di Risi T, Della Monica R, Buonaiuto M, Costabile D, Pisani A, Coccozza S, Chiariotti L. Ultra-Deep DNA Methylation Analysis of

X-Linked Genes: GLA and AR as Model Genes. *Genes (Basel)*. 2020 Jun 4;11(6):620.

IX. Affinito O, Palumbo D, Fierro A, **Cuomo M**, De Riso G, Monticelli A, Miele G, Chiariotti L, Coccozza S. Nucleotide distance influences co-methylation between nearby CpG sites. *Genomics*. 2020 Jan;112(1):144-150.

X. **Cuomo M**, Keller S, Punzo D, Nuzzo T, Affinito O, Coretti L, Carella M, de Rosa V, Florio E, Boscia F, Avvedimento VE, Coccozza S, Errico F, Usiello A, Chiariotti L. Selective demethylation of two CpG sites causes postnatal activation of the Dao gene and consequent removal of D-serine within the mouse cerebellum. *Clin Epigenetics*. 2019 Oct 28;11(1):149.

XI. Pellecchia S, Sepe R, Federico A, **Cuomo M**, Credendino SC, Pisapia P, Bellevicine C, Nicolau-Neto P, Severo Ramundo M, Crescenzi E, De Vita G, Terracciano LM, Chiariotti L, Fusco A, Pallante P. The Metallophosphoesterase-Domain-Containing Protein 2 (MPPED2) Gene Acts as Tumor Suppressor in Breast Cancer. *Cancers (Basel)*. 2019 Jun 8;11(6):797.

XII. Affinito O, Salerno P, D'Alessio A, **Cuomo M**, Florio E, Carlomagno F, Proietti A, Giannini R, Basolo F, Chiariotti L, Coccozza S, Santoro M. Association between DNA methylation profile and malignancy in follicular-patterned thyroid neoplasms. *Endocr Relat Cancer*. 2019 Apr 1;26(4):451-462.

XIII. Coretti L, Paparo L, Riccio MP, Amato F, **Cuomo M**, Natale A, Borrelli L, Corrado G, De Caro C, Comegna M, Buommino E, Castaldo G, Bravaccio C, Chiariotti L, Berni Canani R, Lembo F. Gut Microbiota Features in Young Children With Autism Spectrum Disorders. *Front Microbiol*. 2019 May 3;10:920. doi: 10.3389/fmicb.2019.00920. Erratum for: *Front Microbiol*. 2018 Dec 19;9:3146.

XIV. Keller S, Punzo D, **Cuomo M**, Affinito O, Coretti L, Sacchi S, Florio E, Lembo F, Carella M, Copetti M, Coccozza S, Balu DT, Errico F, Usiello A, Chiariotti L. DNA methylation landscape of the genes regulating D-serine and D-aspartate metabolism in post-mortem brain from controls and subjects with schizophrenia. *Sci Rep*. 2018 Jul 5;8(1):10163.

XV. Coretti L, Cristiano C, Florio E, Scala G, Lama A, Keller S, **Cuomo M**, Russo R, Pero R, Paciello O, Mattace Raso G, Meli R, Cocozza S, Calignano A, Chiariotti L, Lembo F. Sex-related alterations of gut microbiota composition in the BTBR mouse model of autism spectrum disorder. *Sci Rep.* 2017 Mar 28;7:45356.

XVI. Coretti L, **Cuomo M**, Florio E, Palumbo D, Keller S, Pero R, Chiariotti L, Lembo F, Cafiero C. Subgingival dysbiosis in smoker and non-smoker patients with chronic periodontitis. *Mol Med Rep.* 2017 Apr;15(4):2007-2014.

XVII. Coretti L, Natale A, **Cuomo M**, Florio E, Keller S, Lembo F, Chiariotti L, Pero R. The Interplay between Defensins and Microbiota in Crohn's Disease. *Mediators Inflamm.* 2017;2017:8392523.